COMMISSION OF THE
EUROPEAN COMMUNITIES

COOPERATION

Equitable Testing and Evaluation of Marine Energy Extraction Devices in terms of Performance, Cost and Environmental Impact

Grant agreement number: 213380

EquiMar

Deliverable D2.4
Wave Model Intercomparison

Grant Agreement number: 213380

Project acronym: EQUIMAR

Project title: Equitable Testing and Evaluation of Marine Energy Extraction Devices in terms of Performance, Cost and Environmental Impact

Deliverable D2.4

Wave Model Intercomparison

Vengatesan Venugopal and Thomas Davey
University of Edinburgh, UK
Françoise Girard
Actimar, France
Helen Smith
University of Exeter, UK
Luigi Cavaleri, Luciana Bertotti and Mauro Sclavo
CNR-ISMAR, Italy

January 2011

Summary

This report examines the application of a number of numerical wave models to the process of quantifying the resource at a specific coastal site. The models are used to transform the deep water wave climate to a location in shallower water. Validation of the models is conducted using existing wave buoy measurements at the site. The results and analysis presented are intended to give practical insight to the modelling processes involved in a site specific resource assessment. Variations between the models are examined and discussed.

CONTENTS

1 INTRODUCTION

1.1 MODEL INTERCOMPARISON FOR RESOURCE ASSESSMENT

1.1.1 Scope of this Report

This report examines the practicalities of applying a numerical model to transform a wave climate from one location to another. A selection of spectral wave models (SWAN, TOMAWAC and MIKE21) have been employed for this purpose and these models use a common dataset as input driving conditions to provide insight into the comparability and performance of these models. Document D2.3 (*Application of Numerical Models*) gives guidance on the setup, inputs and calibration/validation of numerical models. Some elements of D2.3 are reproduced here for the purposes of background and clarity.

1.2 RESOURCE ASSESSMENT

Marine energy resource assessments may be conducted to various levels of detail depending on the stage of a project or the end user. In particular assessments may be conducted to identify suitable geographic locations for deployment. Once suitable areas have been identified a detailed assessment will be necessary to characterise a particular site. These processes will be referred to as *Resource Characterisation* and *Site Assessment* in the outputs of the EquiMar project.

1.2.1 Resource Characterisation

Resource characterisation is normally carried out to establish suitable geographic locations for deployment, and has the following objectives:

- To ascertain the potential resource for energy production with an explicitly stated degree of uncertainty;
- To identify constraints on resource harvesting.

1.2.2 Site Assessment

Site assessment is normally carried out prior to deployment, to establish the detailed physical environment for a particular marine energy project, with the following objectives:

- To assess the energy production throughout the life of the project;
- To characterise the bathymetry of the site to an explicitly specified and appropriate resolution;
- To ascertain the spatial and temporal variation of the resource with an explicitly stated degree of uncertainty;
- To describe metocean conditions;
- To establish extreme (survivability) conditions with a defined return period;
- To identify potential interference between multiple devices at the site.

Numerical wave modelling plays major role in the above assessments.

1.3 NUMERICAL MODELS FOR RESOURCE ASSESSMENT

Numerical models potentially play several important roles in the assessment of the marine energy resource. For geographical level *Resource Characterisation* a model may be deployed to provide data over a wide area for a statistically significant period of time. This combination of wide spatial and long temporal coverage is generally not feasible by direct measurement. Point measurement devices (e.g. wave buoys) require multiple deployments to provide useful spatial information and long measurement programmes are not economical. Remote measurement devices (e.g. satellites) provide more detailed spatial information but their temporal coverage tends to be sporadic.

Having identified potentially exploitable sites with the aid of the resource characterisation process a more detailed *Site Assessment* must be conducted. This process aims to provide detailed spatial information sufficient for determining the placement of individual devices along with an understanding of the temporal variations expected over the life of the project.

Many sites of interest to the wave energy community are in relatively shallow water in coastal regions. Models deployed in site assessment, and to a lesser extent resource characterisation, may be used to transform data from a well described deep water region to these shallower regions where no measured data is available. The deep water data may be based on physical measurements, a validated global model or a combination of the two. The transformation process is intended to take into account factors such as coastal topography, local bathymetry, wind and current etc.

In addition to the long term predictions numerical modelling may also play a role in short term forecasting, particularly in the field of wave energy. The problems associated with the variable nature of the resource (particularly the supply of electricity to the grid) may be mitigated in part if the output can be predicted several days in advance at a particular marine energy site. A calibrated numerical model, likely supported by on-site measurements, may be capable of providing short term forecasts based upon distant data from measurements or a global model.

2 OVERVIEW OF MODELS

2.1 GENERAL

High quality information is required for energy device planning and installation, both for energy resource assessment and for design purposes. Ideally this information should be provided by specific local measurements. There are, however, obstacles to this approach:

1. Measured local data are scarce and rarely available for the long period required for reliable information
2. Measurement programmes are costly and time consuming.
3. Most local measurement programmes (buoys and ADCPs) provide only point measurements.

Therefore a more cost-effective and spatially extensive data source is required.

Data covering the last 10-20 years are available from satellite remote sensing at a reasonably comprehensive level. However, satellites are available only along predetermined ground tracks, and provide information on the significant wave height and possibly period. Synthetic Aperture Radar (SAR) is, in principle, capable of providing full two-dimensional spectra, but their information is not available, rather sparse, and their accuracy is still highly debated.

The most practical solution to the measurement problem is provided by the results of wave models operational at several meteo-oceanographic centres around the world. These provide, and have provided for many years, continuous spectral information on dense regular grids covering the whole world. They are by far the most complete source of wave information presently available. Suitably validated against buoy and altimeter data, the synergy of these three sources provides the most complete and accurate source of wave data presently available. If buoy measured data are not already available in the specific area of interest, wave model data provides the most reliable form of resource assessment.

Also, data from a calibrated and validated model can be used to bridge gaps in measured data due to the temporary unavailability of the measurement instrument (due to equipment failure, deployment delays etc.). It is also the case that the measurement instrument may not be capable of supplying all the necessary wave output parameters required for different analyses: for example, some particular types of instrument will only provide unidirectional wave spectral parameters, or only a small subset of wave parameters. In situations like this, if one is interested in directional wave properties, it may be possible to derive them directly from a numerical wave model.

Spectral wave models underwent rapid development in the late 1980s and early 1990s, with the introduction of the so-called third-generation models. Unlike previous versions, these models are based uniquely on the physical numerical description of the various processes that occur during the evolution of the sea state. The basic advantage is that, as the physics of wind-waves is the same everywhere, these models can be applied anywhere, with the appropriate bathymetry (grid extension and resolution) and suitable wind data. Highly reliable as they are, the third generation wave models presently in widespread use still show minor differences in their outputs. These differences are related to the different numerics at the base of each model and to possible differences in the physical assumptions expressed in their equations. Therefore, at the preliminary assessment stage (or in a study such as presented here) it is convenient to apply different models in the same area and using the same input. This will give an indication of the reliability of the models, especially when, as in the present study, they are compared to recorded wave data.

Wave propagation models can thus be divided in two major categories:

Deterministic (phase resolving) models are based on a rigorous approximation of the fundamental hydrodynamic equations, and are typically applied in shallow or intermediate water. Their basic characteristic is the capability to translate the elevation time history from one point (the input) to another, providing a continuous high frequency description in space and time of the evolution of the sea surface.

Spectral (phase-averaged) models provide a statistical description of the wave conditions in space and time, typically at the nodes of a grid covering the area of interest. They provide, point by point, the distribution of wave energy in frequency, direction and its evolution in time. Spectral models are commonly divided into three generations:

- **First Generation:** Early models, developed in the 1960s, were designed to model wave energy growth and dissipation. Their major limitation is that they do not account for the nonlinear interactions between the different wave frequencies.
- **Second Generation:** The later generation of models used parameterised approximations to model the nonlinear spectral interactions. Explicit calculation of these interactions is very computationally expensive.
- **Third Generation:** First developed in the late 1980s, these models provide a full description of the physical processes governing wave evolution. This method, while computationally more expensive, requires fewer assumptions on the nature of spectral evolution than the parameterised relationships used in the second-generation models.

In basic terms the deterministic models focus on a specific limited area, with a detailed surface time history at its border. They provide the full time-spatial description of the local sea surface, but are extremely time consuming and generally not user friendly.

Spectral models provide the basic information (significant wave height, direction, peak and mean frequency, plus full spectral energy distribution) required for engineering applications. They are widely available, mostly as open source, and some with a graphical interface allowing use also by non-expert users. They are widely used by both the scientific community and industry.

The information produced during the last 20 years is available mostly at meteo-oceanographic centres, and more recently, results from some EU funded projects (e.g. My Ocean and Globewave) are openly available.

It is clear that, except in some specific cases, spectral models and their related databases provide the most suitable tools to study the long term wave conditions in areas of potential interest and are the focus of this report. Deterministic models may be useful to study specific situations over a very limited area, but the requirement for a deterministic, wave by wave, input should be considered.

In contrast to spectral model, deterministic models are not in routine use and remain an area of considerable research. The models examined in this study are all spectral models in widely used by the marine modelling community.

2.2 WAVE MODELS

2.2.1 Model Summary

The wave models used for the present work are briefly described in Table 1.

Table 1 Summary of selected wave models

SWAN	SWAN is probably the most widely applied model, especially by private and industrial users. The software is **openly available** and very user-friendly. Built originally for research, it offers the possibility of different theoretical approaches to the various processes considered. The default version leads to good results. It works on regular and irregular (finite elements or curvilinear) grids.
MIKE 21	MIKE21 is a 3rd generation spectral wind-wave model developed by DHI, Denmark and is **commercially available**. This model simulates the growth, decay and transformation of wind-generated waves and swells in offshore and coastal areas. The model includes wave growth by action of wind, non-linear wave-wave interaction, dissipation by white-capping, dissipation by wave breaking, dissipation due to bottom friction, refraction due to depth variations, and wave-current interaction. Mike21 is a very user friendly software and works on unstructured mesh grids. A structured mesh is characterized by regular connectivity that can be expressed as a two or three dimensional array. This restricts the element choices to quadrilaterals in 2D or hexahedra in 3D. An unstructured mesh is characterized by irregular connectivity is not readily expressed as a two or three dimensional array in computer memory. This allows for any possible element that a solver might be able to use. Compared to structured meshes, the storage requirements for an unstructured mesh can be substantially larger since the neighbourhood connectivity must be explicitly stored.
TOMAWAC	TOMAWAC one of the modelling software of the TELEMAC system, a processing line designed to study environmental phenomena in free surface transient flows (now openly available). Main scientific areas covered by Telemac are hydrodynamics, sediments transport and wave modelling. Since all the simulation modules of the TELEMAC system are based on the same framework, the coupling of them is easily achieved. Based on unstructured grids, it is suitable for the computation of spectral wave transformations in coastal complex areas It needs development for operational applications.

2.2.2 Modelled Processes

In general spectral models model the following processes:

a) Wave generation by wind
b) Non-linear interaction
c) White capping (breaking in deep water)
d) Bottom friction.
e) Shallow-water breaking (depth induced)
f) Advection
g) Refraction – shoaling

While non-linear interaction (b) is theoretically well defined, all the other listed processes are critically dependent on the input information to the model. Wave generation (a) depends on the wind speed, fetch and duration. White-capping (c) depends on the input wave spectrum. Processes (d) to (g) depends on the bathymetry and on the quality of the bottom characteristics and composition (mainly its material and grain size).

For resource assessment purposes local wave modelling will be applied to characterise a particular site. The actual domain of the model will, however, extend beyond the boundary of site to a point where suitable input information is available. This input

information may take the form of a wave buoy but is more likely obtained from a global wave model. In the following sections we discuss how the accuracy of the results depends on this input information and on modelling of the various processes. The relative importance of these factors is summarised in Table 2.

Table 2 Relative importance of various physical mechanism in different regions of the ocean: 1- negligible; 2- minor importance; 3- significant; 4 – dominant (Battjes, 1994; Young, 1999)

Physical Process	Deep Oceans	Shelf Seas	Shoaling Zone	Harbours
Diffraction	1	1	2	4
Depth refraction/shoaling	1	3	4	3
Current refraction	1	2	3	1
Quad Interactions	4	4	2	1
Triad Interactions	1	2	3	2
Atmospheric Input	4	4	2	1
White-capping	4	4	2	1
Depth Breaking	1	2	4	1
Bottom Friction	1	4	2	1

2.3 WAVE MODELLING OVERVIEW

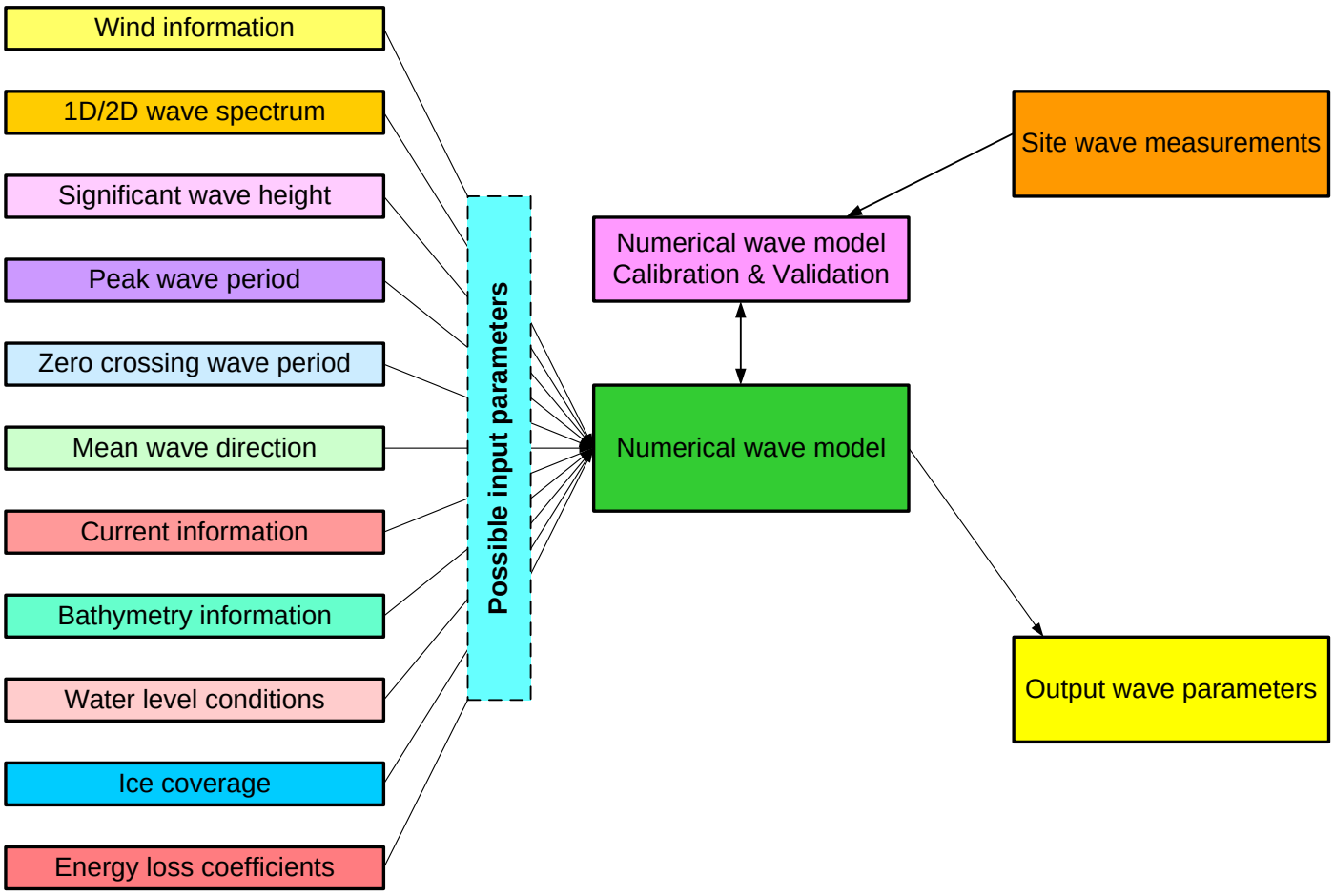

Figure 1 Schematic representation of numerical wave modelling process

A schematic representation of wave modelling procedure is illustrated in Figure 1. The setup procedure, required by every numerical model, involves transforming the real world data into a format that can be easily recognisable by the wave model. As a first step, a computational domain has to be chosen with boundaries (dimensions) on all four sides defined. The domain should be setup with a mesh (structured or unstructured) and bathymetry which are essential to obtain reliable results for the computational area selected for investigation. Sufficient accuracy should be maintained in specifying the bathymetry as this has large influence on wave transformation. Also a proper resolution in the mesh selected is important as this affects the stability considerations. The accuracy in the resulting output parameters from a model depends on the accuracy with which the input parameters used at the model boundaries. Most of the errors in third generation wave models come from the errors in the input data, connected both to their resolution and accuracy. One of the most frequent sources of errors is the wind (related to the high sensitivity of the wave results to the driving wind field). Much attention must be paid to the resolution of both the wind data and the wave model grid used to model the area. This resolution must be able to resolve the details, for example of the bathymetry or of the local wind and wave spatial gradients. The input parameters (e.g., wind, wave spectrum, current, water level etc) can be specified as a constant value over the computational domain or time, or these can also be used as variable with space and time. Depending on the setup of the models, different offshore input wave conditions are required, ranging from the simple integrated wave parameters, e.g. significant wave height, mean and peak periods, mean direction and the full two-dimensional (2D) spectra. Through a range of possible intermediate solutions, the most complete input information is provided by the 2D spectra, i.e. by the full distribution of the wave energy in frequency and direction (typically between 600 and 900 numbers). These spectra are initially available at the resolution of the large scale model, and therefore before their modelling use they need to be interpolated at the outer points of the local grid one would like to work with.

Similar to the offshore wave data, wind information may be derived from the long-term activity of some operational centre. Ideally one would like to access high resolution wind data that are likely to be more accurate, especially at the small scale, than the global models. However, these data are generally not available when working with historic data. While they are suitable for some specific test in the present time, they are not available for the past. Hence one must resort to the use of global scale modelled

winds. For the tests described in this document, the wind information from the European Centre for Medium-Range Weather Forecasts (ECMWF, Reading, U.K.) has been used, which are available at six-hour intervals.

Once the model is ready with all necessary input information, the simulated results for the first run from the model has to be calibrated with known measurements, so that the model parameters can be tuned to reproduce the known conditions at any site. The tuned model should again be run and the output must be validated with the known measurements. The calibration and verification procedure can be repeated by tuning the relevant model parameters till a satisfied comparison is reached with the site measurements.

3 MODEL INTERCOMPARISON AT FIGUEIRA DA FOZ, PORTUGAL

3.1 SUMMARY

A selection of spectral models (SWAN, TOMAWAC and MIKE21) were used to analyse wave transformation process at Figueira da Foz on the the Portuguese coast (see Figure 2). Buoys deployed during the WAVEMOD project in the mid 1990s were used to provide the input and calibration/validation data. The wave climate at the outer buoy (70m water depth) was transformed to the shallow water buoys located in water depths of 20 m and 12.5 m over a distance of approximately 15 km. Publicly available and propriety bathymetry was used as was wind data from ECMWF (European Centre for Medium-Range Weather Forecasts).

Figure 2 Location of wave modelling site at Figueira da Foz, Portugal.

3.2 SITE SUMMARY

3.2.1 Bathymetry

Bathymetry data was extracted from publicly available datasets held by the National Oceanic and Atmospheric Administration's (NOAA, USA) ETOPO1 global grid and the GEBCO_08 (GEneral Bathymetric Chart of the Oceans) dataset available from the British Oceanographic Data Centre (BODC). These datasets are both available for free download (for use within the terms and conditions of the respective institutes). The resolution is 30 arc-second and 1 arc-minute for the GEBCO_08 and ETOPO1 grids respectively. The GEBCO bathymetry is illustrated in Figure 3. Whether this level of detail (i.e. 30 arc-second resolution) is sufficient will depend on the purpose of the modelling. In the case of a high level, geographical scale, resource assessment the resolution is likely to be sufficient. When the locations of the buoy deployments are examined in more detail (~30km x 30km grid) it is noted that some detail is lost in shallow water, particularly when examining the coastline.

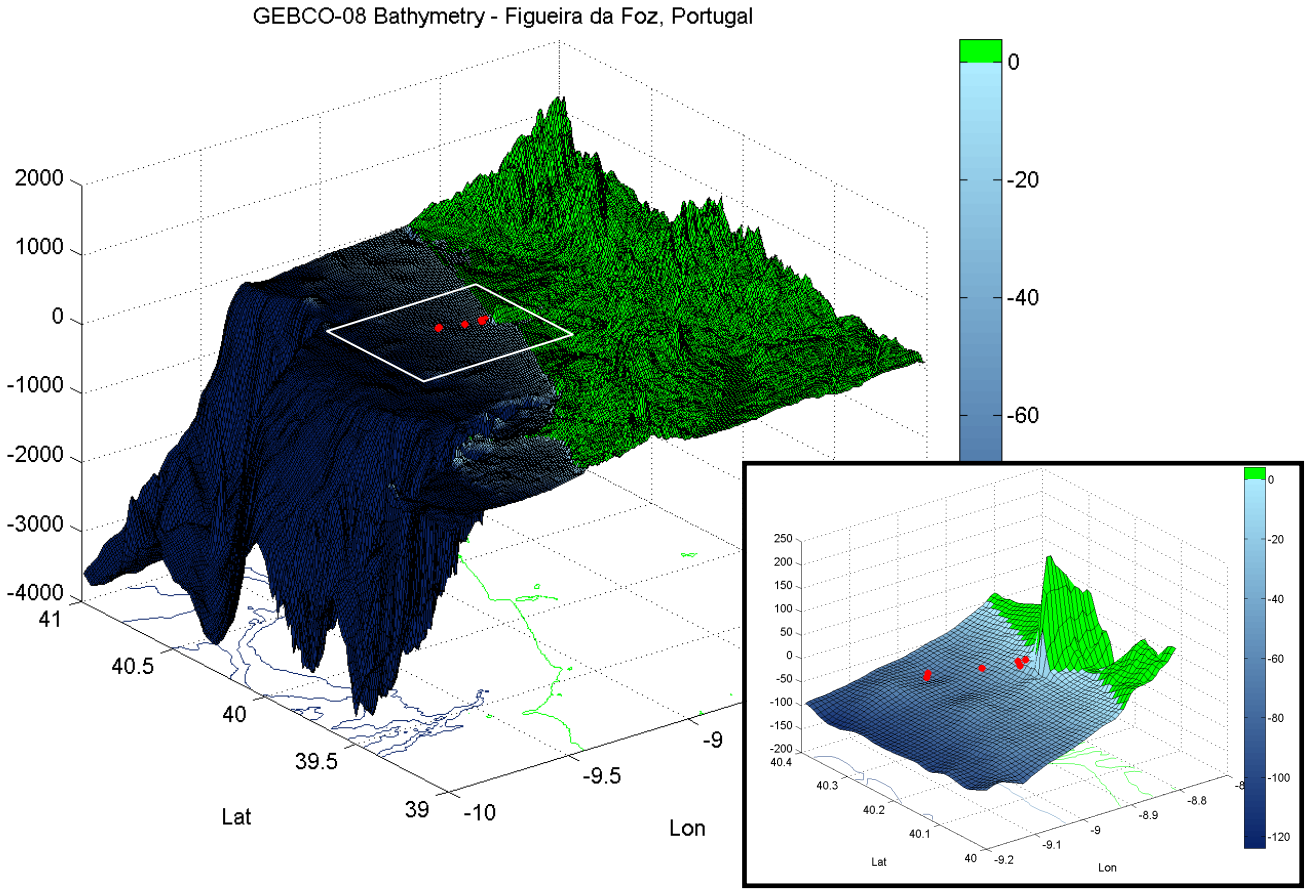

Figure 3 GEBCO_08 30 arc-second resolution bathymetry for Figueira da Foz, Portugal. Red markers indicate previous wave buoy deployments. Scale indicated depth in metres.

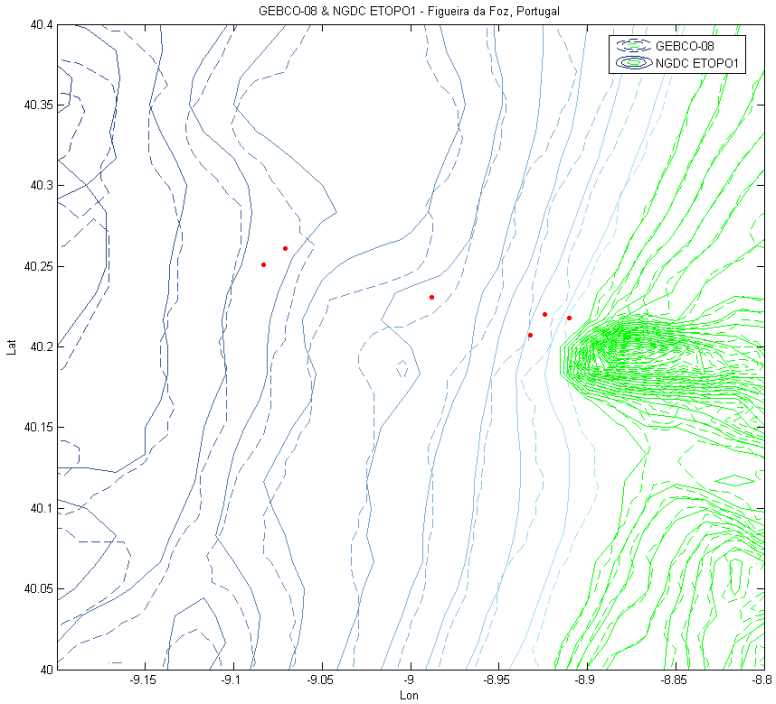

Figure 4 Comparison of GEBCO_08 and NOAA ETOPO1 bathymetry at Figueira da Foz, Portugal. Contours at 8m intervals.

A comparison of the GEBCO and ETOPO1 datasets at the Figueira da Foz site (Figure 4) shows differences between the datasets which, although small in magnitude, are significant. This is especially true in the shallowest water. Comparing the depths with the measured depth at the wave buoys showed an average disagreement in the order of 3-5 metres.

It is recognised that the resolution of the GEBCO and ETOPO1 datasets are lower than would be ideally required for a detailed site assessment. Commercial datasets offer higher resolution data in coastal regions. One such electronic commercial version of the chart, C-Map, is provided through Jeppesen Norway's electronic chart database (http://www.jeppesenmarine.com/). The Danish Hydraulic Institute produced a software module known as MIKE C-MAP which process the C-Map charts and extracts bathymetry for a desired location. The bathymetry prepared for the Figueira da Foz site using MIKE C-Map is shown in Figure 5. The comparison of commercial data with the GEBCO and ETOPO1 datasets has not shown any pronounced differences.

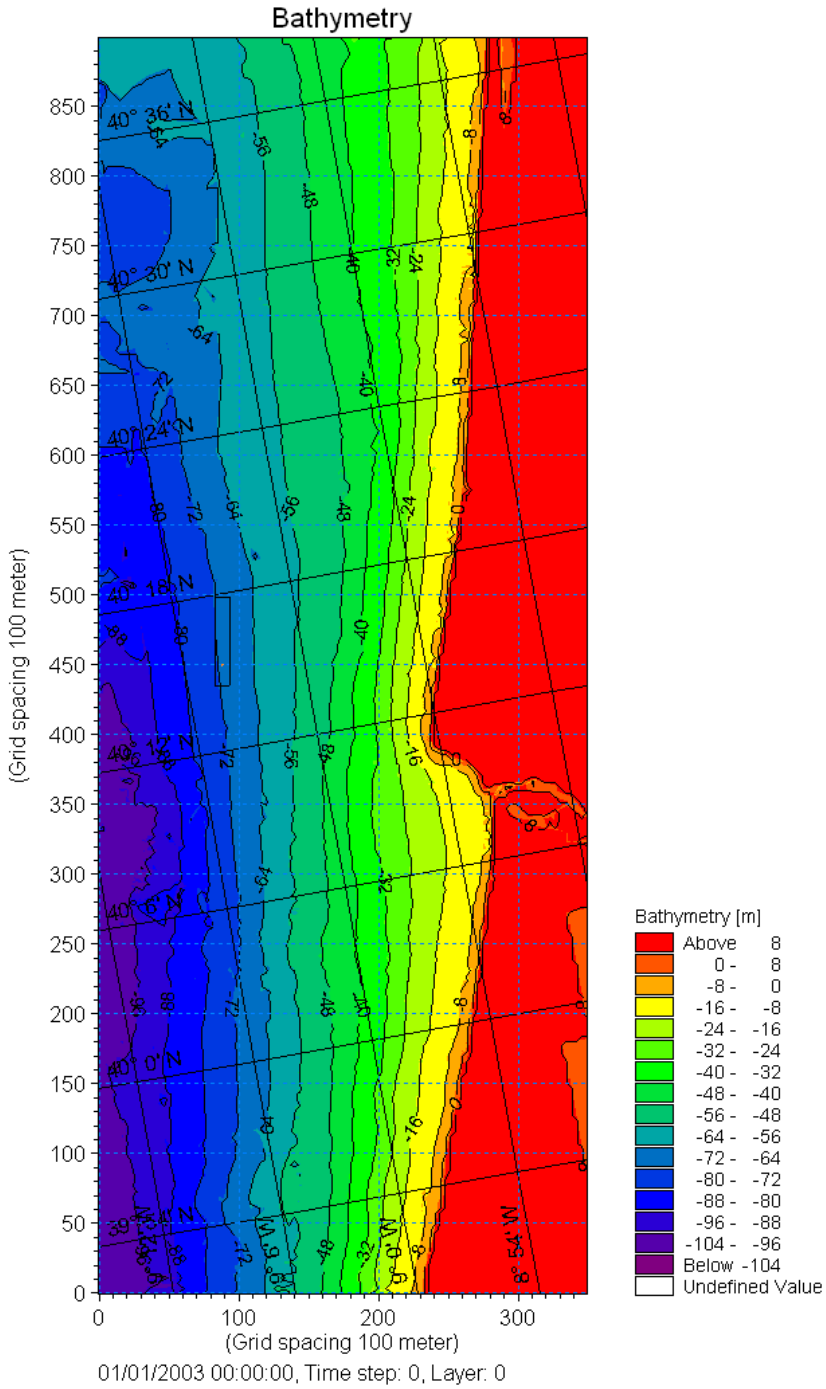

Figure 5 Bathymetry for Figueira da Foz site, Portugal, produced from the commercial charts

3.2.2 WAVEMOD Programme

The site at Figueira da Foz offers a rare combination of buoys located concurrently at several water depths. The buoys were deployed during 1993-1994 for the purposes of the MAST WAVEMOD project. The buoys were deployed in two phases, with 3 buoys being deployed at any one time. The positions of these buoys during the two phases are illustrated in Figure 6. Further details are given in Table 3. The measurements taken during Phase 2 of the programme were used for modelling purposes.

Figure 6 Wave buoys located off the coast of Figueira da Foz, Portugal

Table 3 Summary of wave buoys at Figueira da Foz, Portugal

Project Phase	Water Depth [m]	Position	Deployment Start	Deployment End	Directional [Y/N]
1	19.6	40.220°N, -8.924°E	19/10/1993	04/03/1994	Y
	49.7	40.232°N, -8.988°E	19/10/1993	12/01/1994	N
	72.1	40.261°N, -9.071°E	19/10/1993	04/03/1994	Y
2	12.5	40.218°N, -8.910°E	04/03/1994	01/05/1994	N
	19.7	40.207°N, -8.932°E	04/03/1994	25/05/1994	Y
	72.1	40.251°N, -9.083°E	04/03/1994	25/05/1994	Y

3.3 SWAN MODELLING WITH UNSTRUCTURED GRIDS

The SWAN model may be run using a regular or unstructured grid. SWAN wave modelling with an unstructured computational grid is described in this section and with the regular grid approach presented in §3.4.

3.3.1 Model Setup

The SWAN model was setup on a grid with triangular elements for comparison with TOMAWAC modelling.

For this purpose, NOAA-NGDC ETOPO1 bathymetry dataset was used with a resolution of 1 arc-minute. The bathymetry roughly agreed with water depth on buoy positions of Mast Wavemod project. The water depth on buoy positions was added to the MNT (see Figure 7). The unstructured grid was composed with 2419 points and 4638 triangular elements.

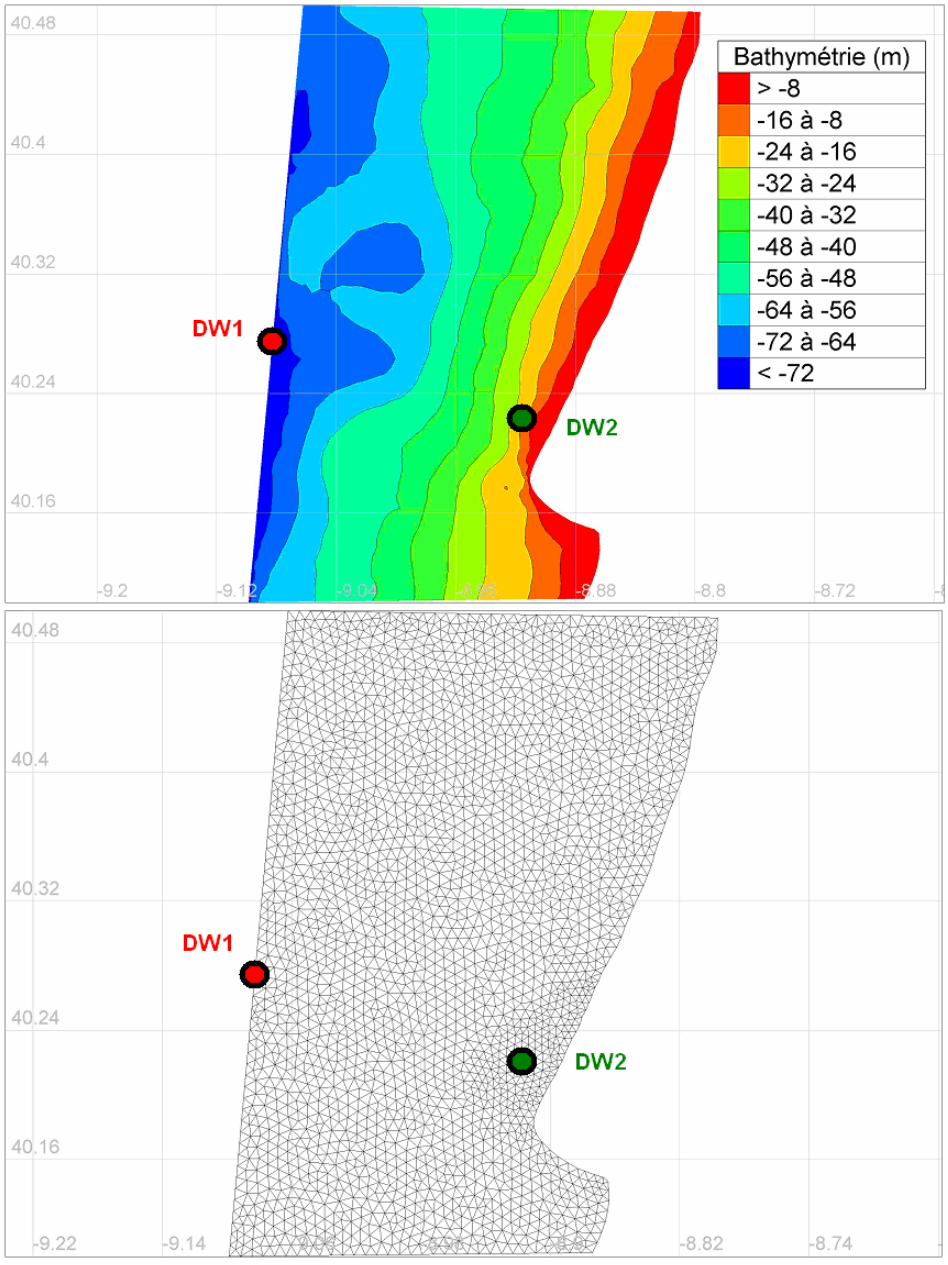

Figure 7 Bathymetry (top) and unstructured mesh (bottom), describing the neighbourhood of Figueira da Foz

Boundary conditions:

Mast Wavemod data are 1D (one-dimensional) spectra with information on directional spreading (Fourier coefficients of the directional distribution). The 2D spectra were recomposed from this information to prepare the input files for spectral modelling. Also, the spectra needed to be re-sampled in frequency, and this was done using a logarithmic scale

$$f^N = r^{N-1} f_1 \quad (1)$$

where r is the ratio of the geometric progression (r = 1.1) is and f_1 is the initial frequency and equal to 0.035 Hz. The computational spectral grid was based on 30 frequencies and 48 directional components. Obviously, some distortion is expected to occur after spectral re-interpolation. Missing data points (error value) in the time series are re-estimated thanks to nearest data.

.

A sample offshore wave spectrum is shown in Figure 8 for March 21 - 16:00, 1994. The left side polar plot shows the input spectrum imposed on offshore boundaries and the right hand polar spectrum is the SWAN model output at the DW1 buoy position. Energy propagation from eastern directions vanishes in SWAN output since it leaves the computational grid.

Processes and parameters:

The SWAN model was run in two stages, one without the effect of wind (no wind forcing) on wave propagation and another including wind effect on wave propagation. The processes shoaling, refraction, bottom dissipation and wave breaking were included in the modelling. When wind forcing was applied, the input wind data obtained from the hindcast data provided by the ECMWF was used. The runs were made with SWAN default parameters.

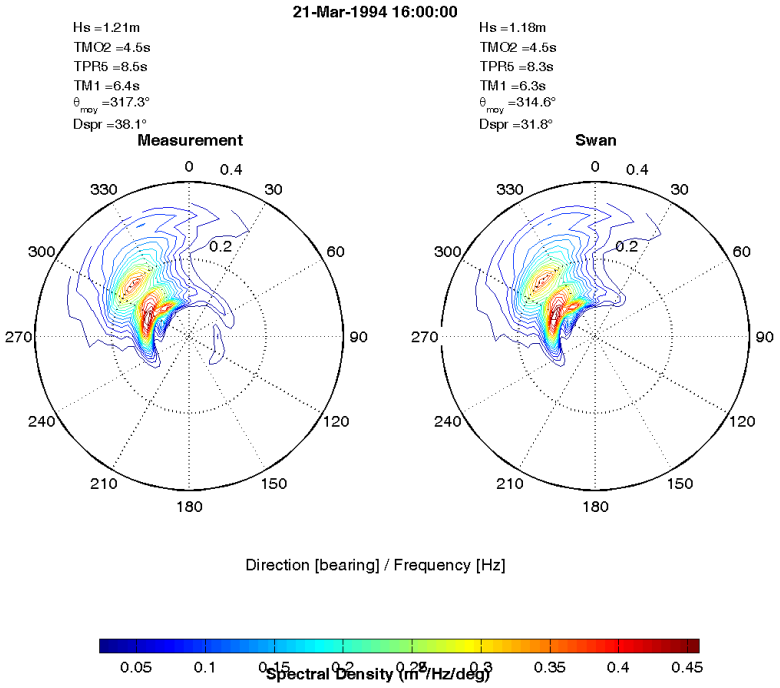

Figure 8 Offshore wave spectrum on 21/03/94 at 16 :00: Measurement and SWAN model

3.3.2 Model Output

3.3.2.1 Significant wave height

The evolution of significant wave height (H_{m0}) is shown in Figure 9 for the period March 5th to May 26th for the offshore buoy (DW1 - 70m) and near shore buoys (DW2 - 20m / DW3 – 12 m). The measured significant wave height is indicated by the red coloured line and SWAN model output significant wave height is by the blue line. These results are corresponding to computations without wind forcing.

Note that buoy DW3 is not a directional buoy and its frequency sampling is 0.5 Hz instead of 3.84 Hz for DW1 and DW2. This means that the highest frequency component of measured waves (frequency cut off) is f_c=0.25 Hz for DW3 (T_{meas}>4 s) compared to f_c=1.92 Hz for DW1 and DW2 (T_{meas}>0.5 s). The high frequency part of the energy spectrum is missing on DW3, but is included in SWAN results (see selected spectra on Figure 11). To improve the comparison on DW3 position, the wave parameters are also computed from SWAN spectra, by considering a frequency cut-off of 0.24 Hz. The results are presented by the cyan coloured line on the temporal plots. Truncation of the spectrum at 0.24 Hz does not impact significantly the results for H_{m0} on DW3.

The plots (Figure 9) indicate that for DW2 (at 20m water depth) and DW3 (at 12m water depth), the model slightly underestimates the significant wave height, more specifically for the highest sea states. Additional computations were made by including the wind forcing. The corresponding results for the significant wave height (H_{m0}) are shown in Figure 10, for the period March 5th to May 26th for DW2 and DW3. The results are compared as scatter plots in Figure 12 and Figure 13 respectively for DW2 and DW3 with 'wind' and 'without wind forcing'. This comparison show a slightly increased scattering when wind forcing is considered in the modelling, however, the overall difference is not significant as the fetch is not very large.

It is evident from Figure 12 and Figure 13 that the correlation between measurement and model is excellent as indicated by a high correlation coefficient of above 0.96 and a RMSE (root mean square error) in the range [0.22m – 0.26 m].

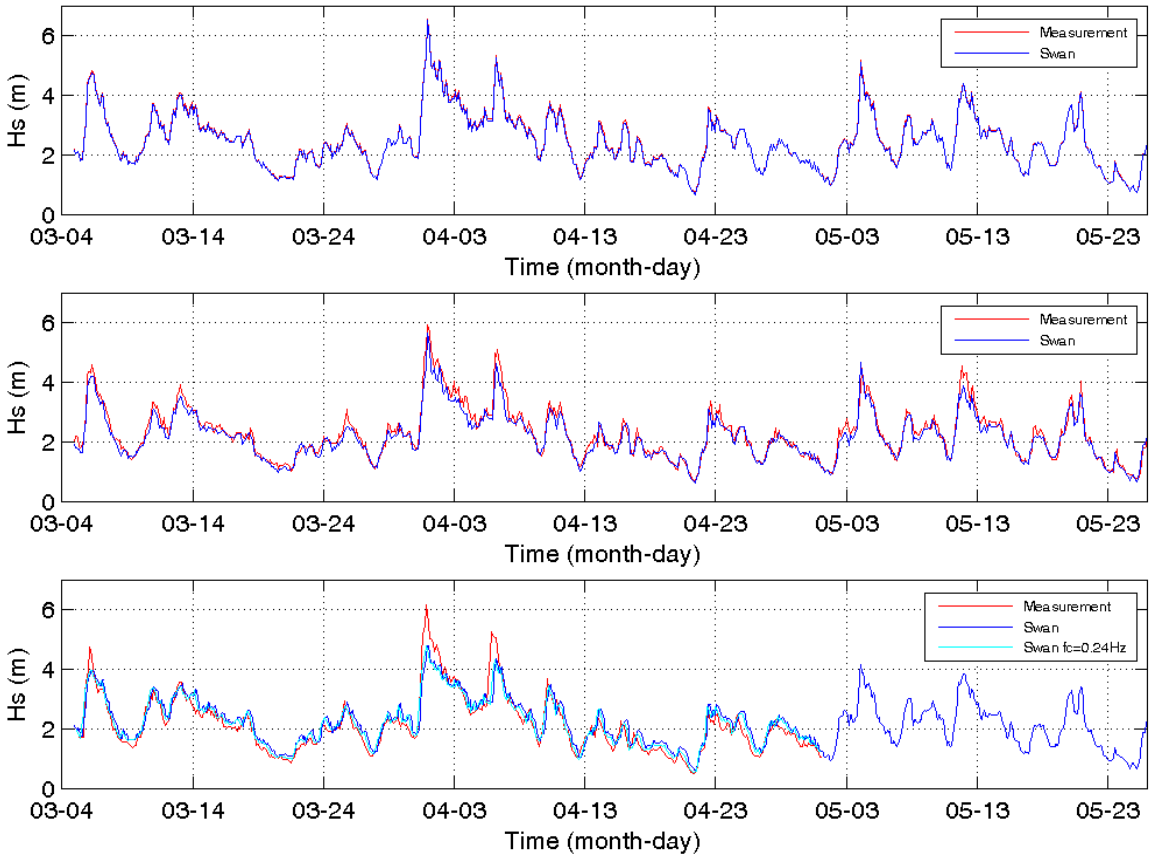

Figure 9 Significant wave height time series: (i) Buoy DW1 offshore buoy (at 70m depth) – upper plot, (ii) Buoy DW2 (20m water depth) – middle plot, and (iii) Buoy DW3 (12 m depth) – bottom plot. The wind forcing is not included in the modelling.

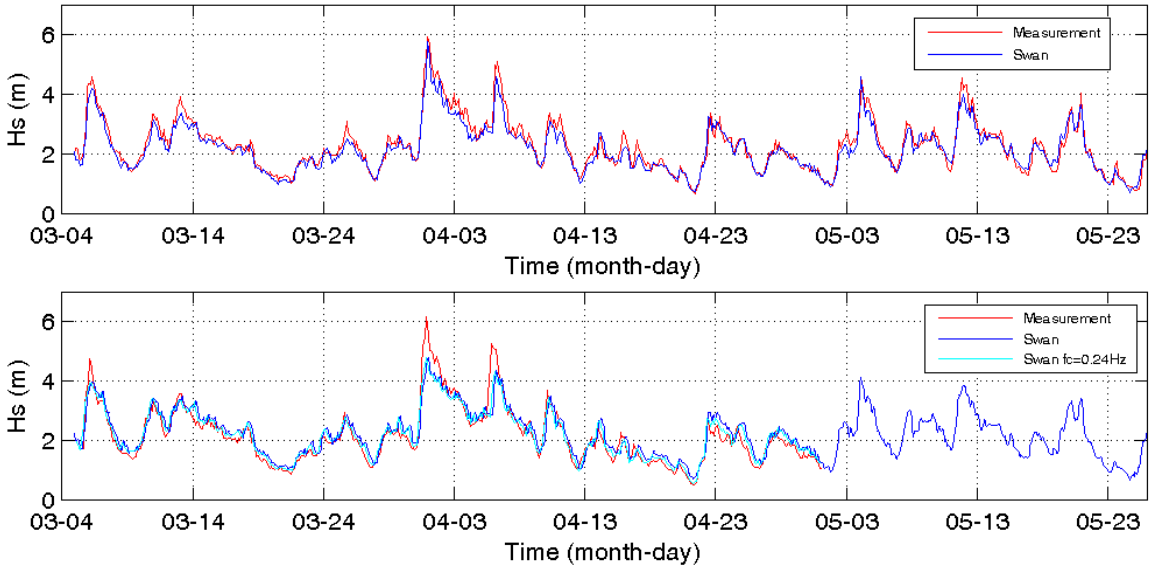

Figure 10 Significant wave height time series: (i) Buoy DW2 (20m depth) – top plot and (ii)) Buoy DW3 (12m depth) – bottom plot. The wind forcing is included in the modelling.

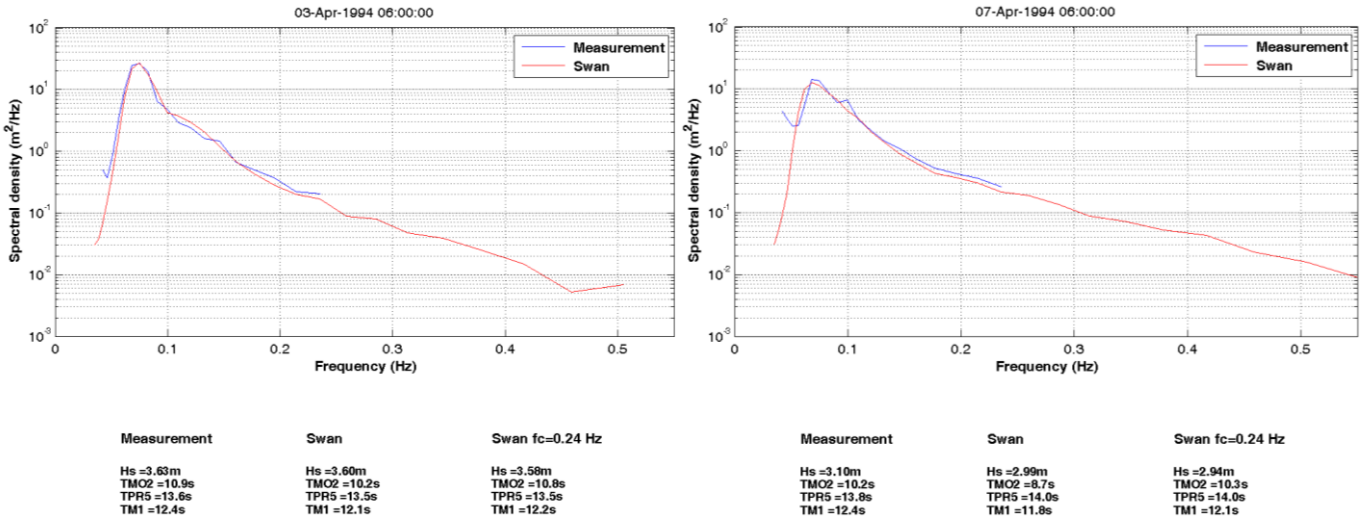

Figure 11 Frequency wave spectra on April 1994. Measurement on DW3 (f<0.24 Hz) and SWAN model.

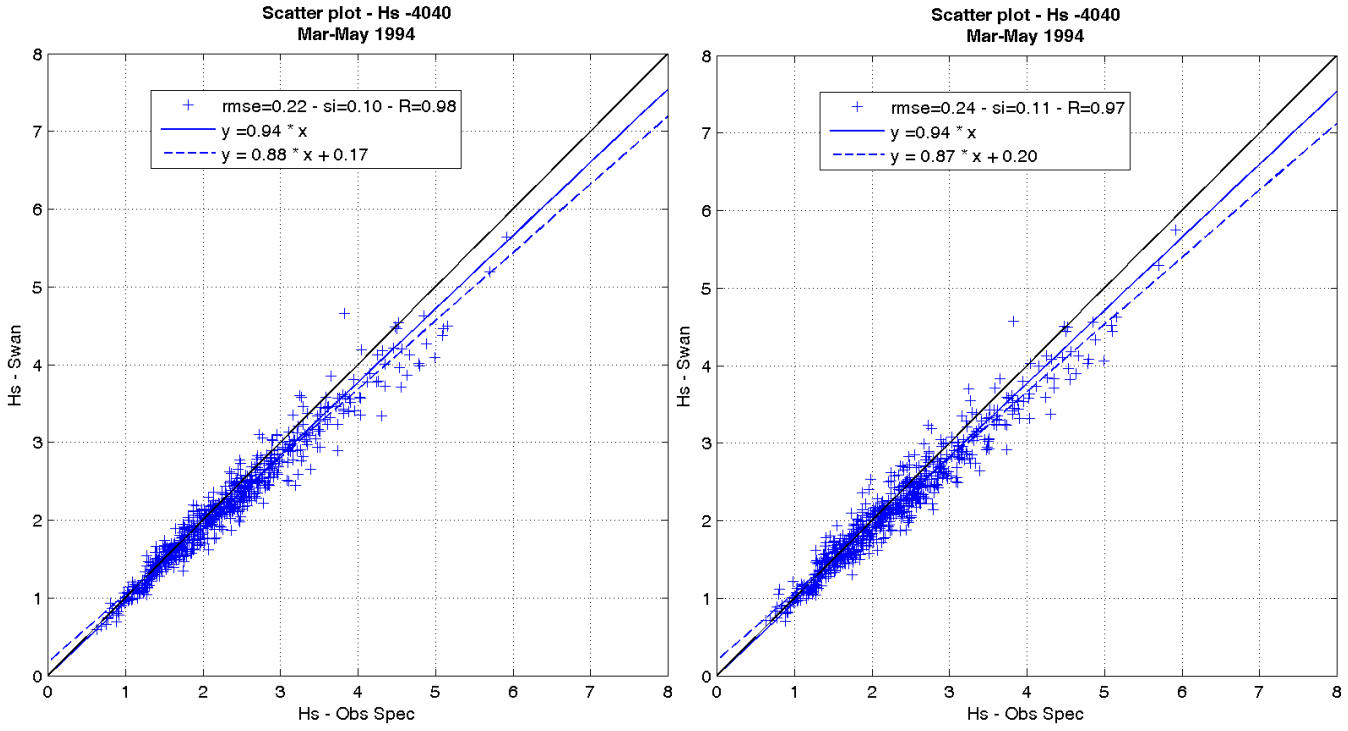

Figure 12 Comparison of Significant wave height between measurements and SWAN model for Buoy DW2: The left hand plot is for 'no wind' and the right hand plot is for 'wind input' included in the model.

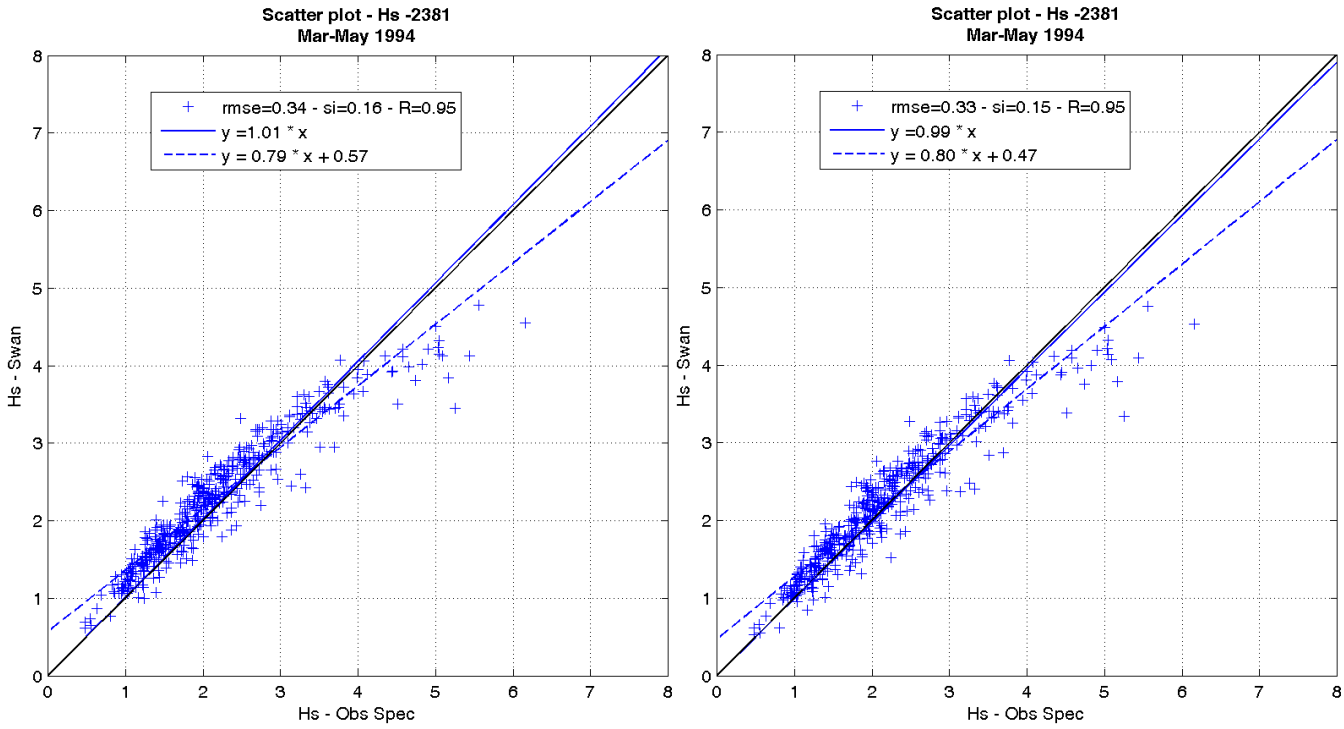

Figure 13 Comparison of Significant wave height between measurements and SWAN model for Buoy DW3: The left hand plot is for 'no wind' and the right hand plot is for 'wind input' included in the model.

3.3.2.2 Mean wave direction

The time series of measured and computed mean wave directions (no wind included into modelling) are shown in Figure 14 for two buoys DW1 and DW2. The results for mean wave direction when wind was input into the model are shown in Figure 15. The comparisons (scatter plots) between measured mean wave direction and model observation with and without wind input are shown in Figure 16. A correlation coefficient of 0.98 was obtained when no wind was input into the model for the buoy DW2, however including the wind input has not increased the correlation, instead it produced a bit higher scatter and increased the RMSE.

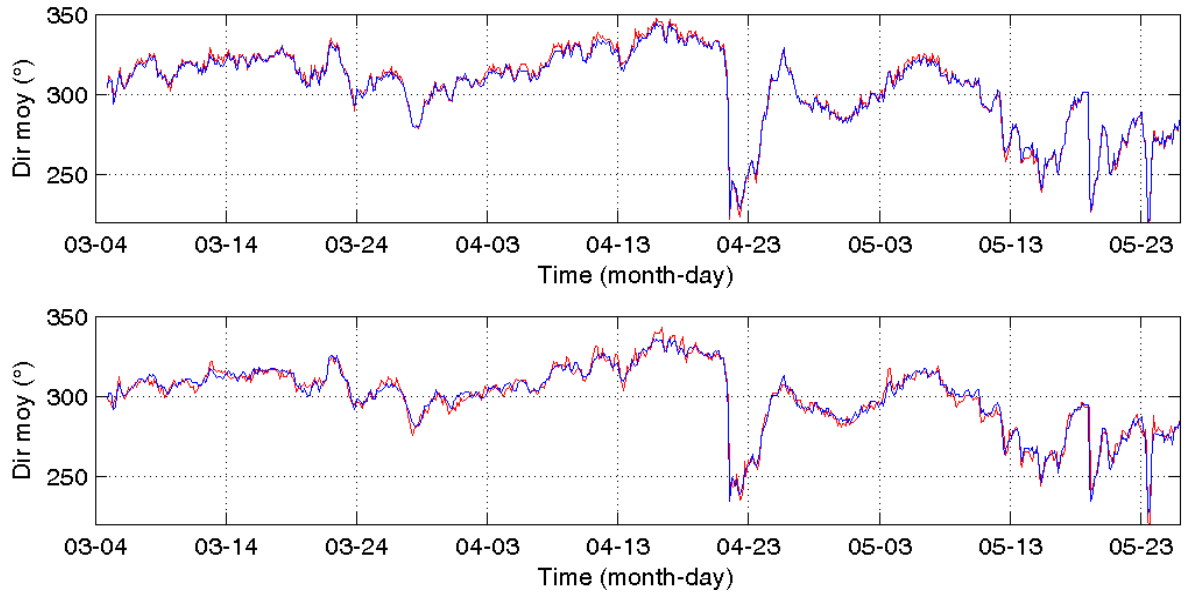

Figure 14 Time series of Mean wave direction: (i) Buoy DW1 offshore buoy (at 70m depth) – upper plot, (ii)) Buoy DW2 (20m water depth) – bottom plot. The wind forcing is not included in the modelling.
Measurement -red, SWAN modelling – blue

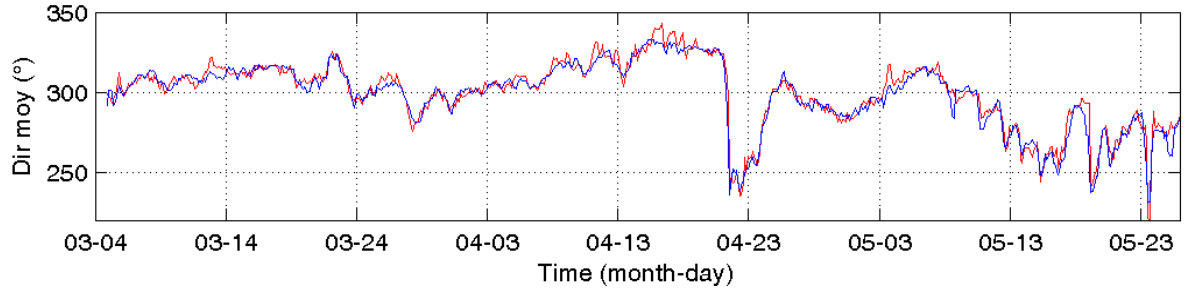

Figure 15 Time series of Mean wave direction: Buoy DW2 (20m water depth). The wind forcing is included in the modelling. Measurement -red, SWAN modelling - blue.

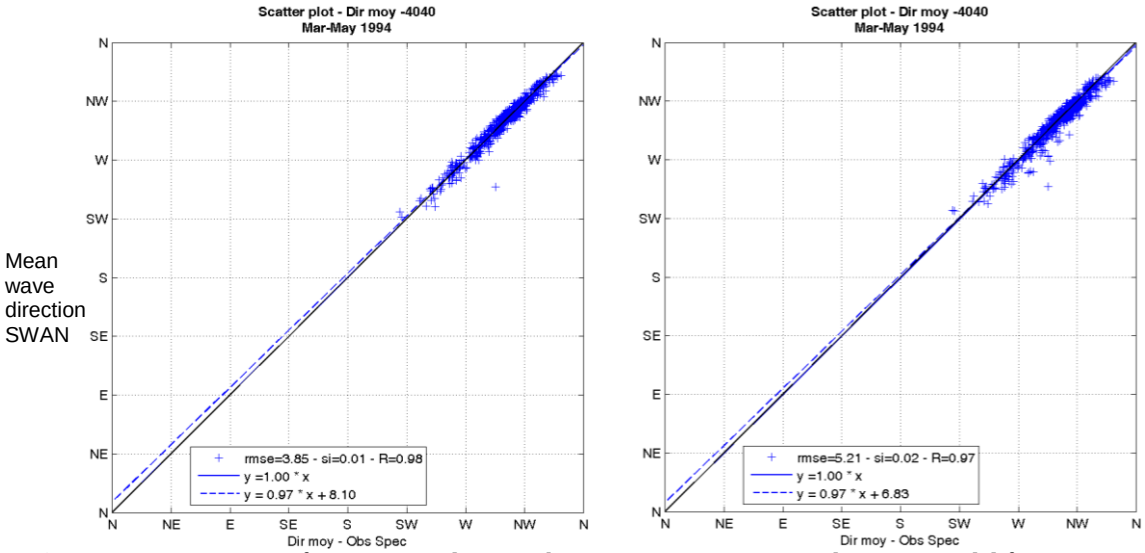

Figure 16 Comparison of Mean wave direction between measurements and SWAN model for Buoy DW2: The left hand plot is for 'no wind' and the right hand plot is for 'wind input' included in the model.

3.3.2.3 Wave Periods (Tp and Tm02)

The peak wave period (T_p) and mean wave period (T_{m02}) from measurements and SWAN model are shown in Figure 17 and Figure 18. As explained in §3.3.2.1, to improve the comparison on DW3 position (frequency sampling reduced to 0.5 Hz) the wave parameters (here T_{m02}) are also computed by considering a frequency cut-off of 0.24 Hz in the output spectra. These results are presented by the cyan coloured line on the temporal plots. In these plots, there are differences between measurements and model output:

- T_p is a parameter evolving rapidly and irregularly when the spectrum is composed of various swell components or when energy on swell and wind sea components are nearly balanced: the maximum of energy may swap from one component to another one. Temporal evolution of T_p on DW2 from April 15th to April 20th illustrates the swap of energy peak between swell and wind sea components. Modelling gives smoother values of T_p.
- Truncation of the spectrum at 0.24 Hz impacts significantly T_{m02} values on DW3. Comparison between measurement (red line) and standard SWAN T_{m02} outputs (blue line) shows a bias which disappears when truncating the modelled spectra (cyan line).
-

The correlation plots on DW2 are presented in Figure 19 and Figure 20. The measured peak wave period deviates significantly from the 'line of equality', showing a large scatter, indicated by RMSE between 1.42 s and 1.47 s and *R* values around 0.88 to 0.89. Again, including wind input into the model has less effect on T_p as indicated by the small *R* value (= 0.89). However, with regard to zero crossing period T_{m02}, SWAN produced an excellent correlation (R = 0.96) with measurements when the wind input was absent. When wind was added to the model, it appears that it influences the zero crossing period largely, yielding a large scatter associated with a less correlation (R = 0.89).

Similar results are observed for Buoy DW3 in Figure 21 and Figure 22, with the exception that including wind has less effect on outputs.

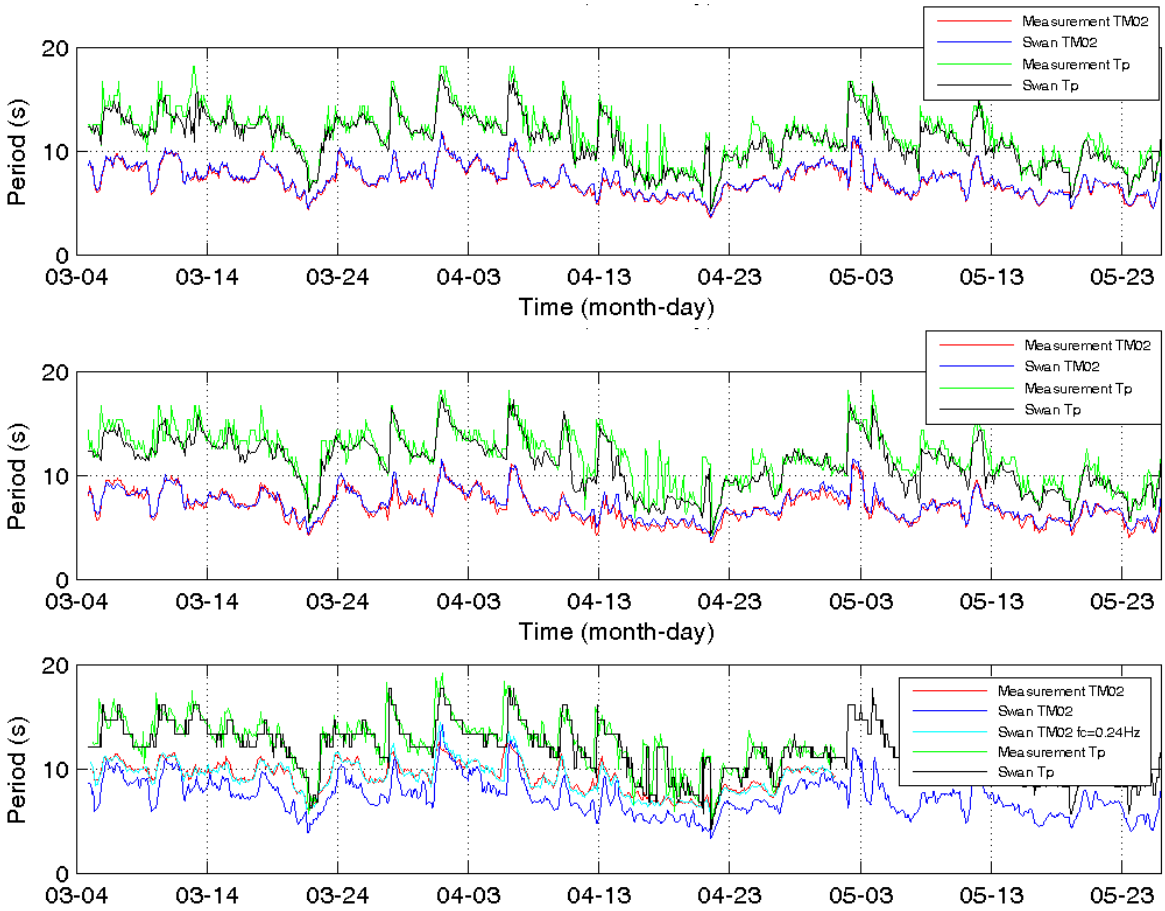

Figure 17 Zero crossing wave period (T_{m02}) and peak wave period (T_p) time series: (i) Buoy DW1 offshore buoy (at 70m depth) – upper plot, (ii) Buoy DW2 (20m water depth) – middle plot, and (iii)) Buoy DW3 (12 m depth) – bottom plot. The wind forcing is not included in the modelling.

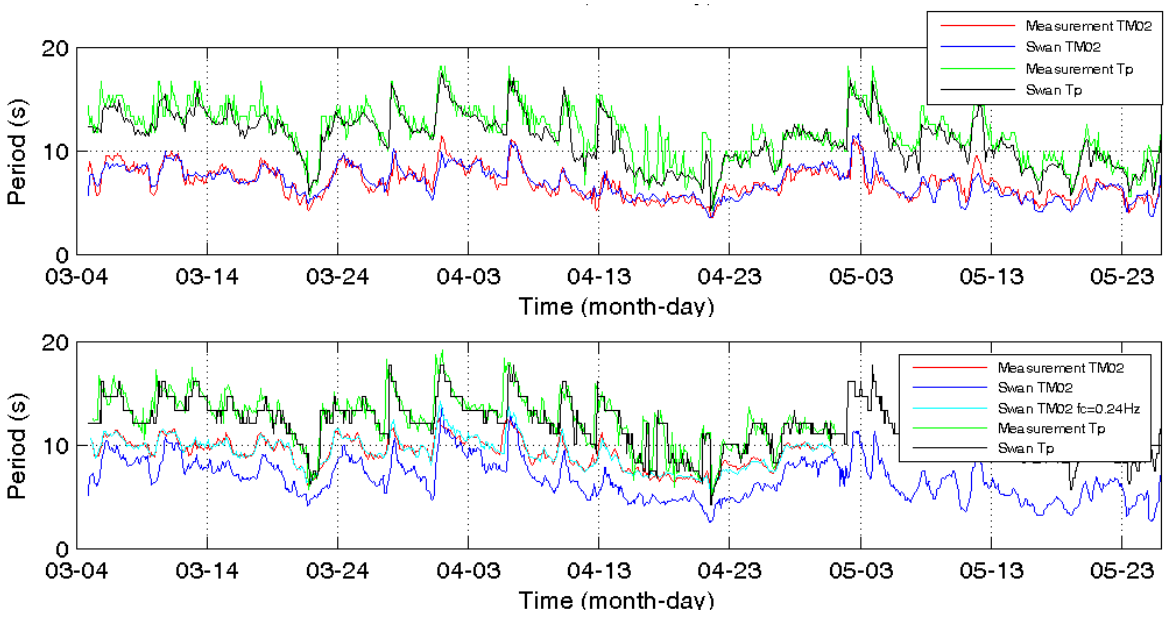

Figure 18 Zero crossing wave period (T_{m02}) and peak wave period (T_p) time series: (i) Buoy DW2 (20m depth) – top plot and (ii) Buoy DW3 (12m depth) – bottom plot. The wind forcing included in the modelling.

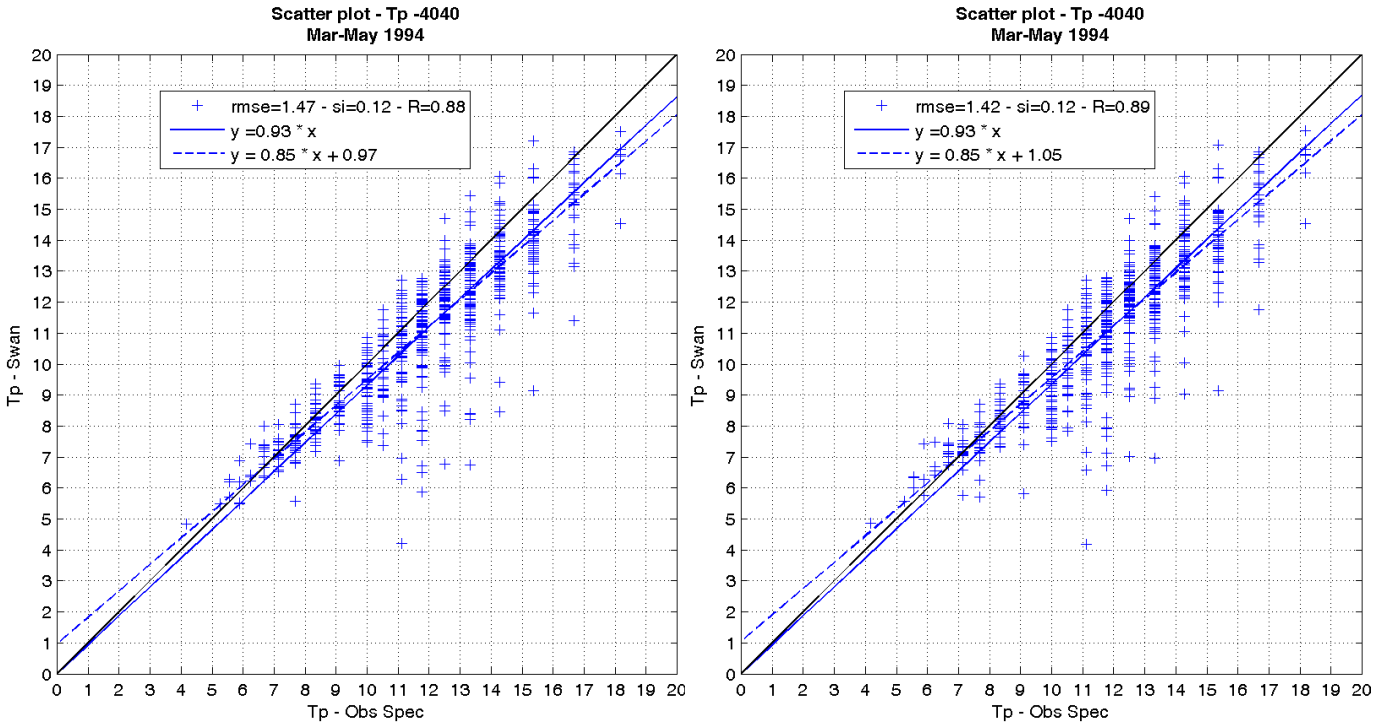

Figure 19 Comparison of peak wave period (T_p) between measurements and SWAN model for Buoy DW2: The left hand plot is for 'no wind' and the right hand plot is for 'wind input' included in the model.

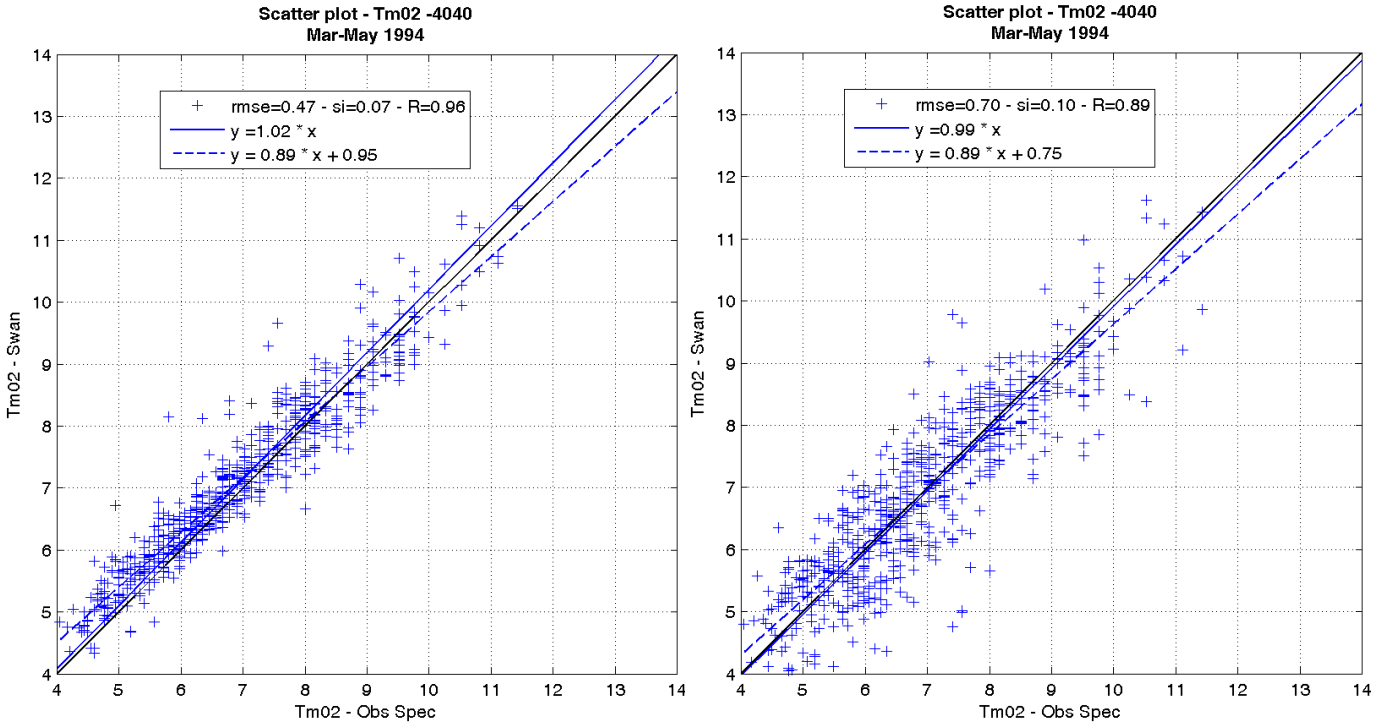

Figure 20 Comparison of zero crossing wave period (T_{m02}) between measurements and SWAN model for Buoy DW2: The left hand plot is for 'no wind' and the right hand plot is for 'wind input' included in the model.

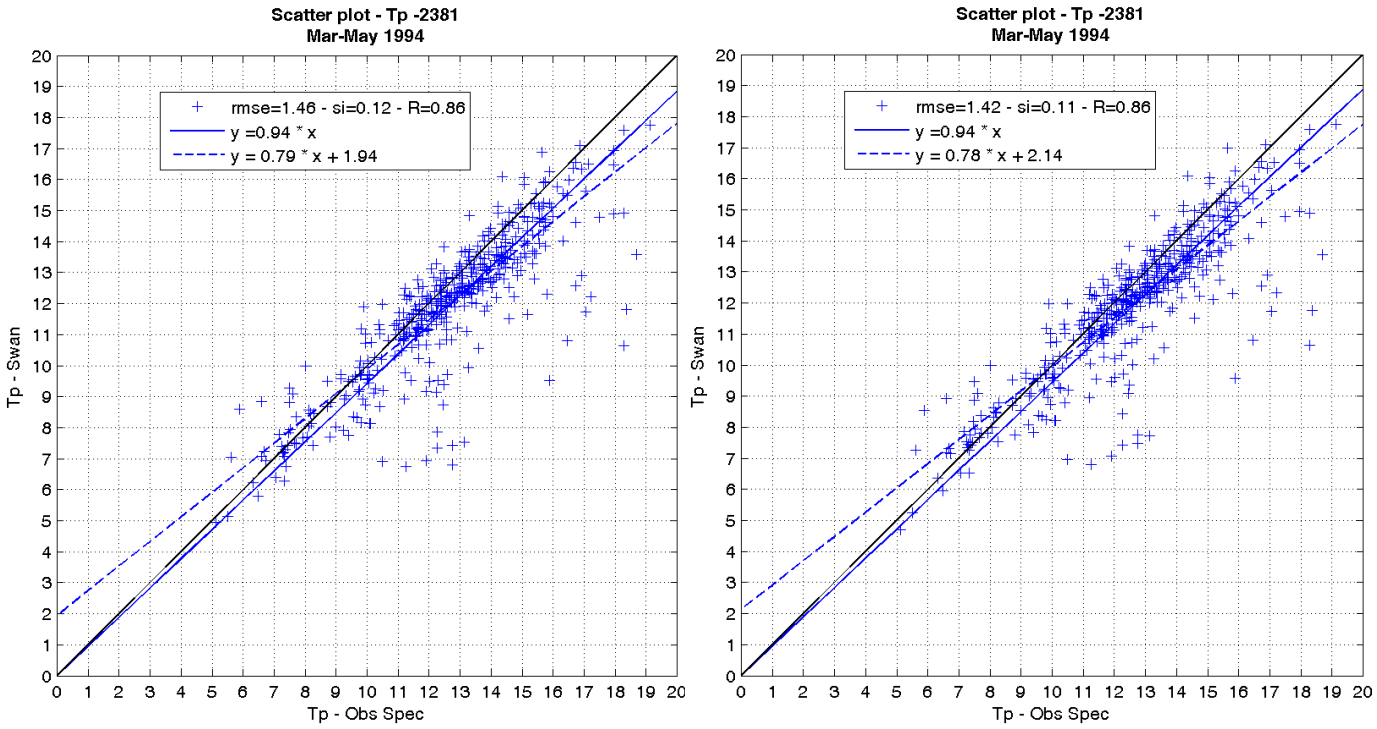

Figure 21: Comparison of peak wave period (T_p) between measurements and SWAN model for Buoy DW3: The left hand plot is for 'no wind' and the right hand plot is for 'wind input' included in the model.

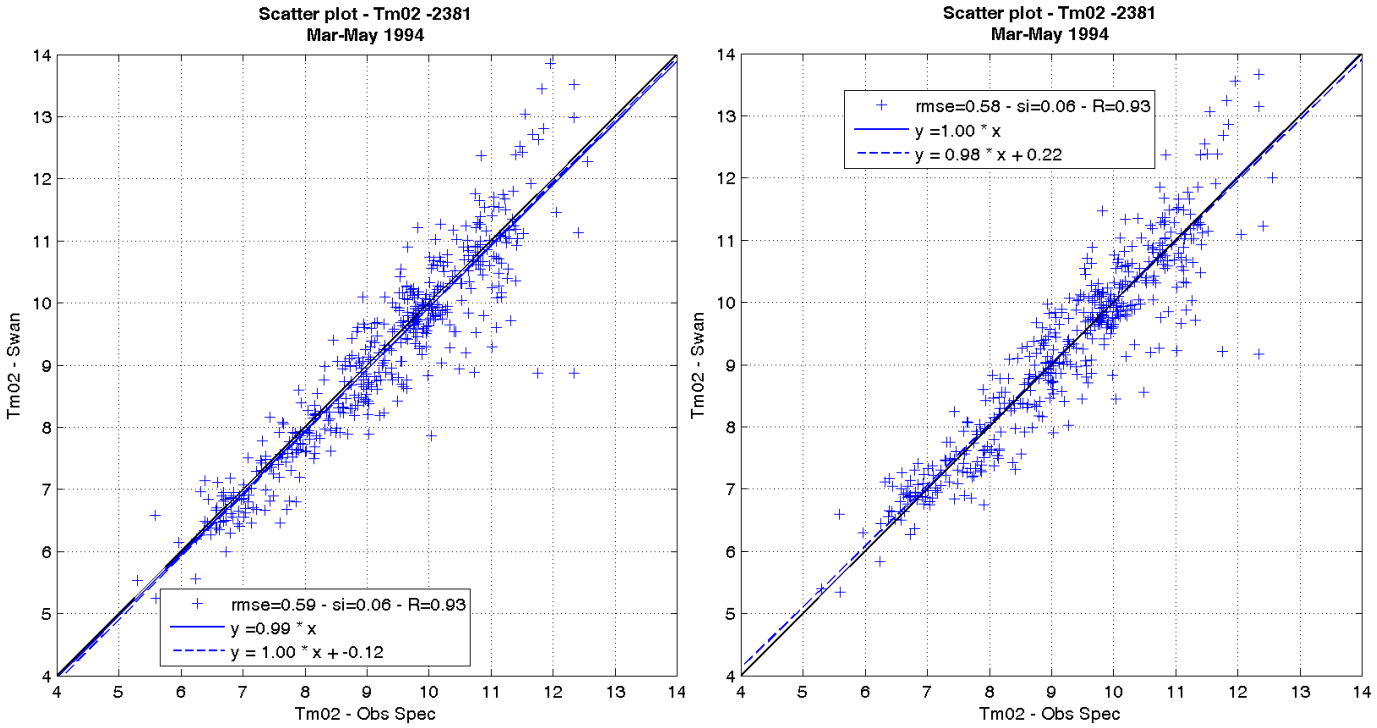

Figure 22 Comparison of zero crossing wave period (T_{m02}) between measurements and SWAN model for Buoy DW3: The left hand plot is for 'no wind' and the right hand plot is for 'wind input' included in the model.

3.4 SWAN Modelling With Structured (Regular) Grids

3.4.1 Model Setup

A regular bottom grid with spherical coordinates was defined from the ETOP01 dataset. A one minute (1/60th degree) resolution at this latitude produces a model mesh size of approximately 1400m x 1850m, a very coarse resolution to be using for a nearshore region such as this. The model domain used for this study is shown in Figure 23. It can be seen that for the region of interest, the contour lines run parallel to the coast and thus the low resolution of the bathymetry may be of less importance than for a region with complex bathymetry. The offshore model boundary was taken along the longitude position of the 70m-depth buoy (9°5'). The model domain was extended as far as possible in the northerly and southerly directions to minimise errors at the model boundaries.

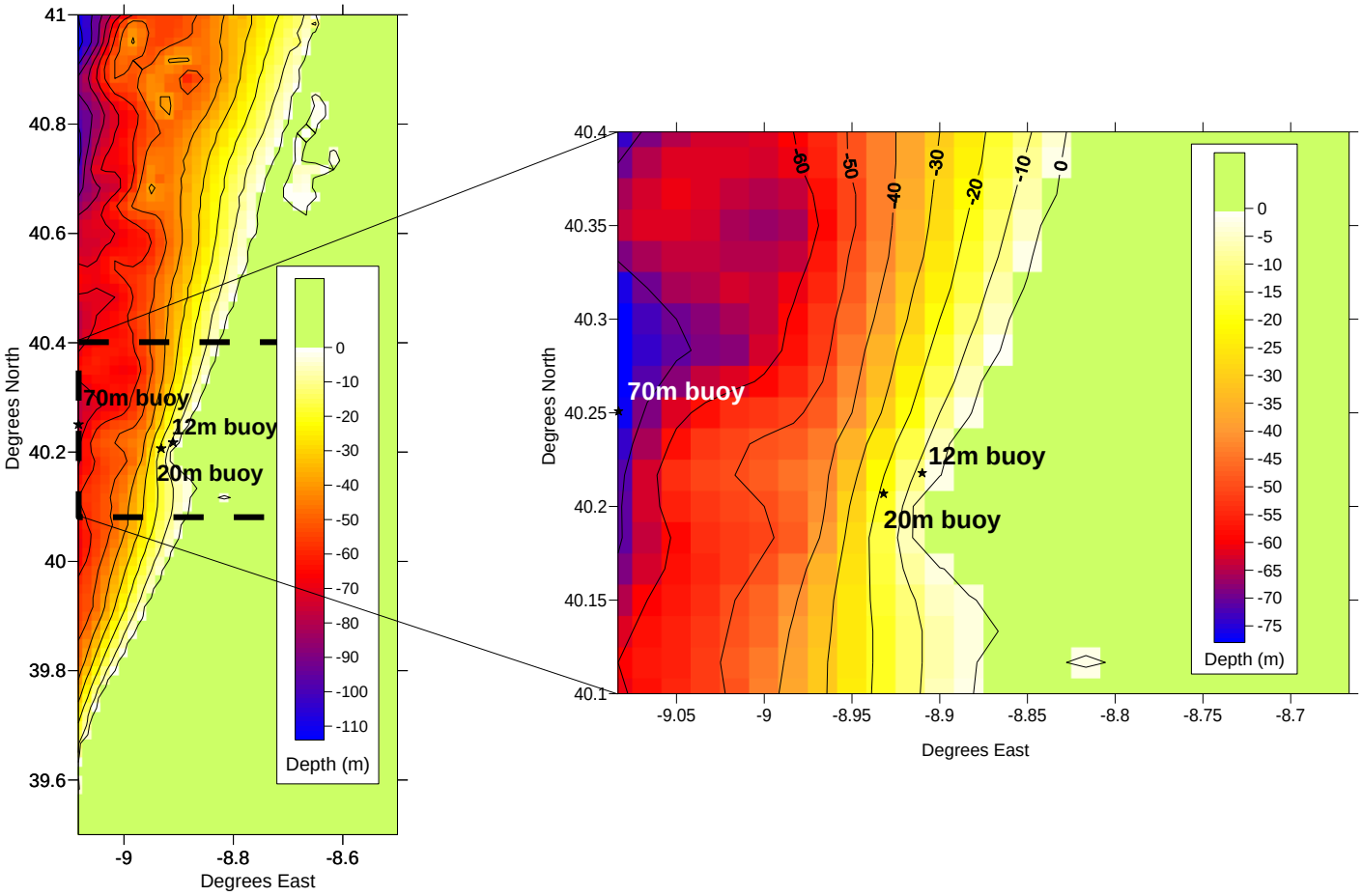

Figure 23 The regular gird SWAN model domain, showing the area of interest in greater detail.

For this study, three sets of constant boundary conditions were input along the offshore model boundary:

- Input 1: Integrated parameters (H_{m0}, T_{m01}, D) from the 70m buoy, fitted to a Pierson-Moskowitz spectrum
- Input 2: 1D spectral input from the 70m buoy
- Input 3: 1D spectral input from the 70m buoy, with a constant wind field applied across the model domain.

The 1D spectra were defined over the frequency range 0.04 – 0.5Hz, with the standard logarithmic frequency distribution for SWAN. The model was run using default values for the user-tuneable parameters. Bottom friction and triad interactions were activated for all runs, with quadruplet interactions additionally activated for the third set of runs with wind input. The model was run in stationary mode using sea states at three-hourly intervals over the period 4/3/94 – 26/5/94. Any missing or erroneous sea states were ignored.

3.4.2 Model Output

The outputs from the model were directional spectra and integrated parameters (significant wave height, zero-crossing period and mean direction), at the locations of the 70m, 20m and 12m buoys, to enable comparisons to be made. The following sections present comparisons between the output parameters (H_{m0}, T_{m02} and D) and the buoy-recorded data at each of the three locations.

The results are shown in Figure 24 to Figure 39.

Significant wave height

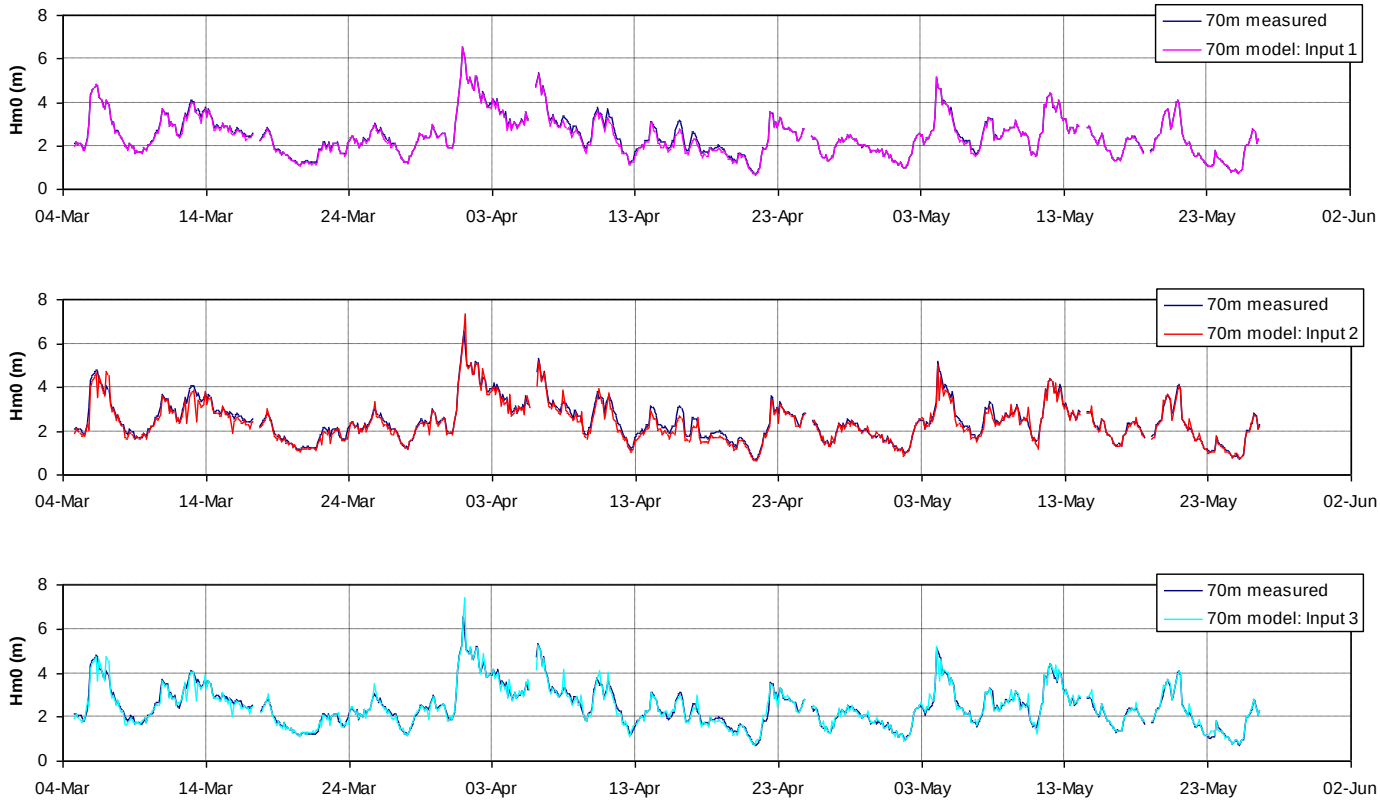

Figure 24 Time series comparison between modelled and recorded H_{m0} at the 70m buoy location for the three types of model input.

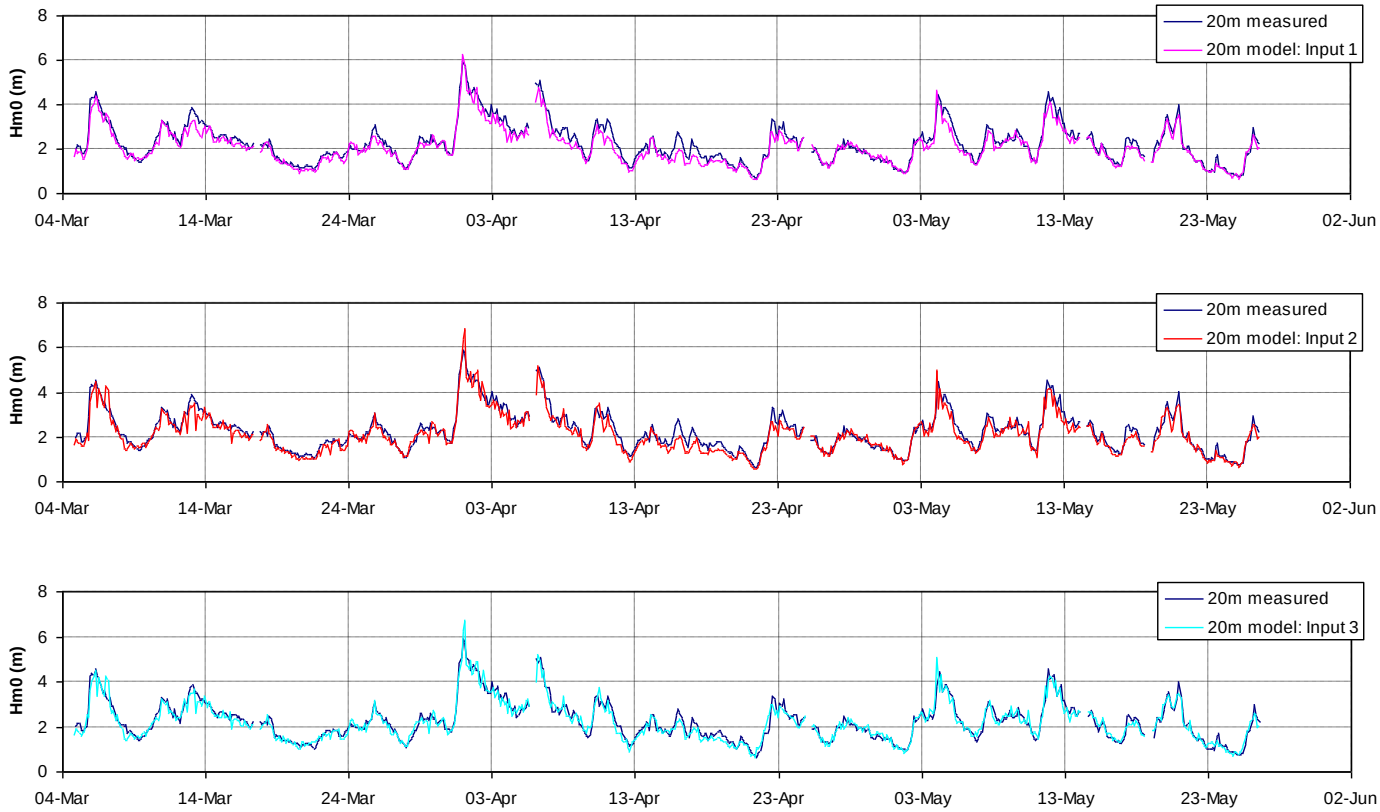

Figure 25 Time series comparison between modelled and recorded H_{m0} at the 20m

buoy location for the three types of model input.

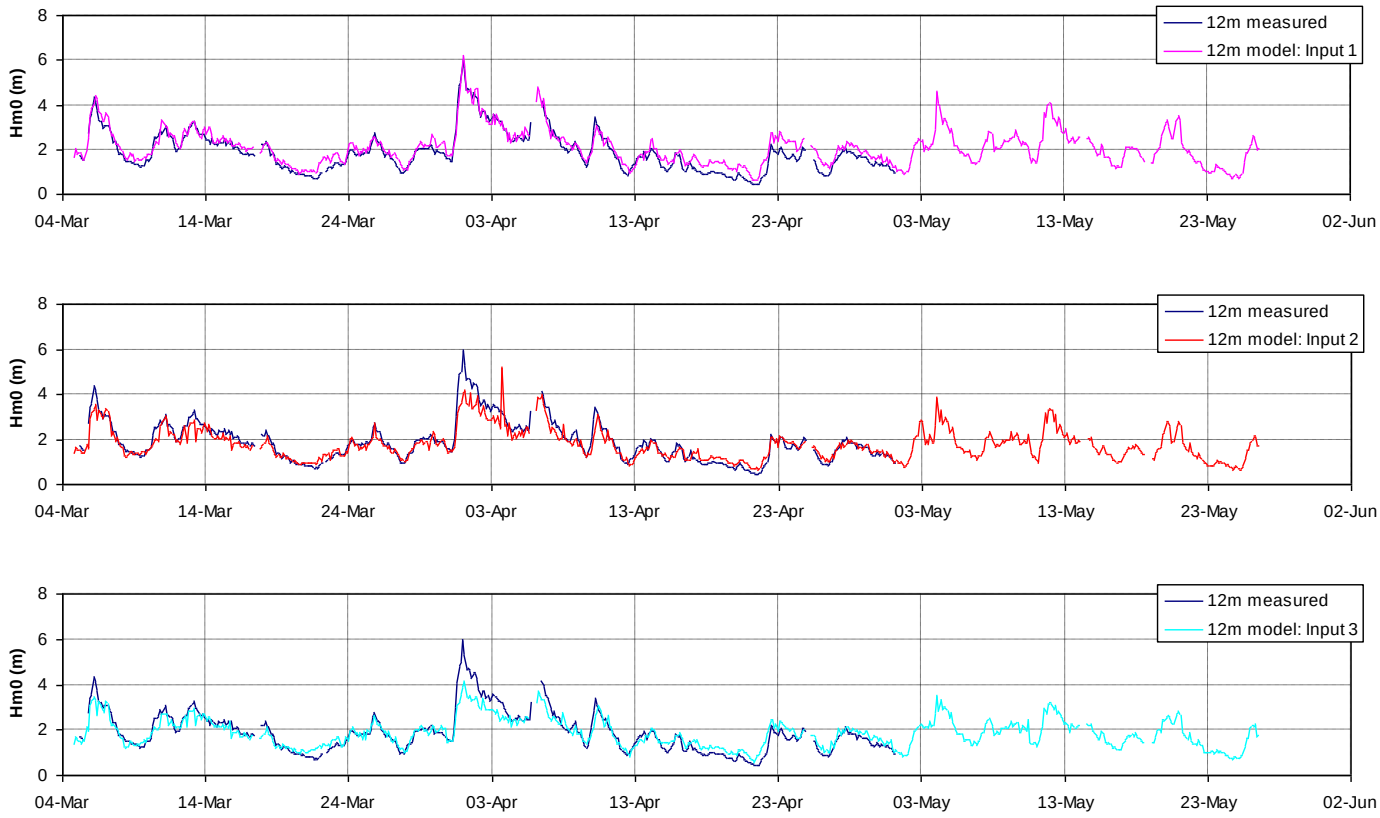

Figure 26 Time series comparison between modelled and recorded H_{m0} at the 12m buoy location for the three types of model input. **Note:** A spike may be observed on the results obtained using Input 2. This anomaly may be attributed to numerical instability in the model.

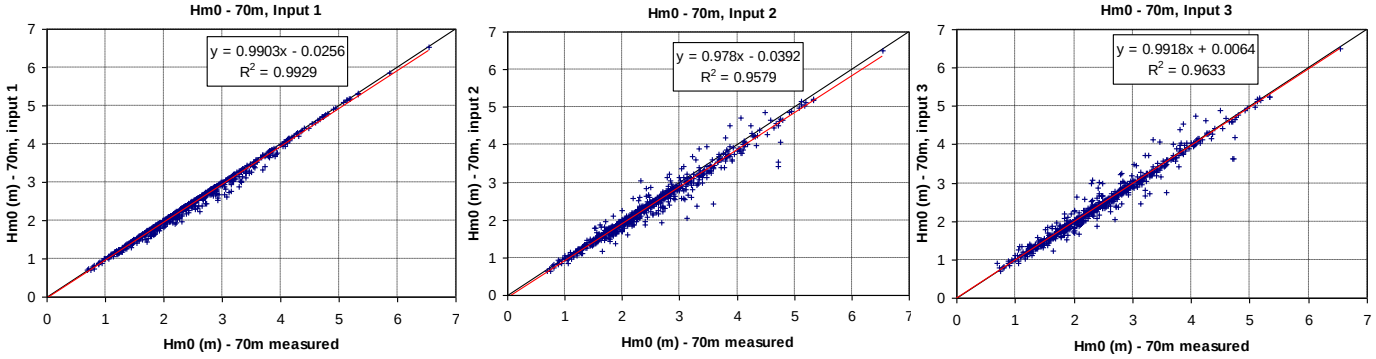

Figure 27 Scatter comparison between modelled and recorded H_{m0} at the 70m buoy location for the three types of model input.

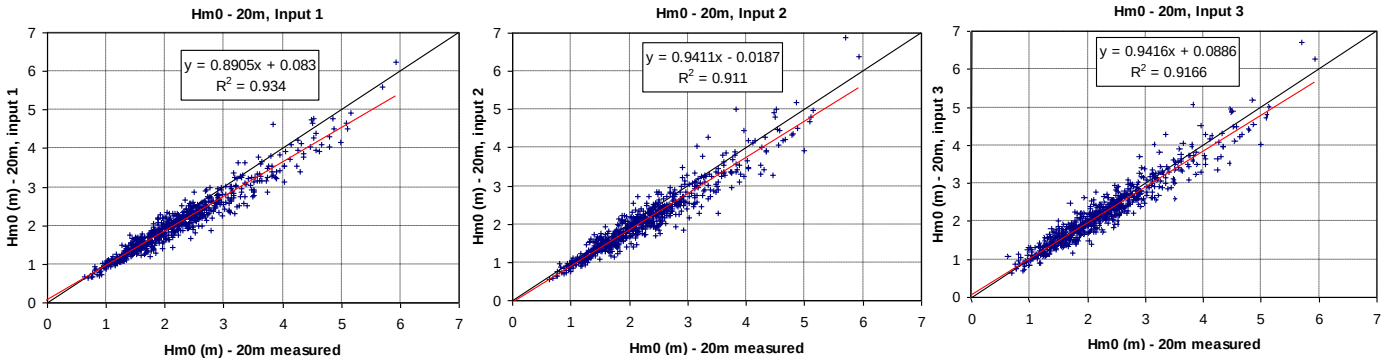

Figure 28 Scatter comparison between modelled and recorded H_{m0} at the 20m buoy location for the three types of model input.

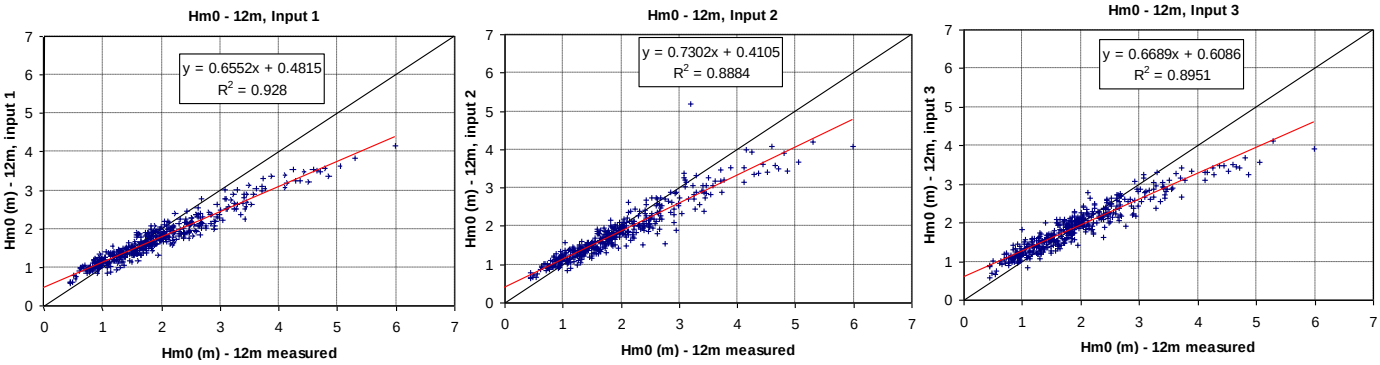

Figure 29 Scatter comparison between modelled and recorded H_{m0} at the 70m buoy location for the three types of model input.

Mean Period

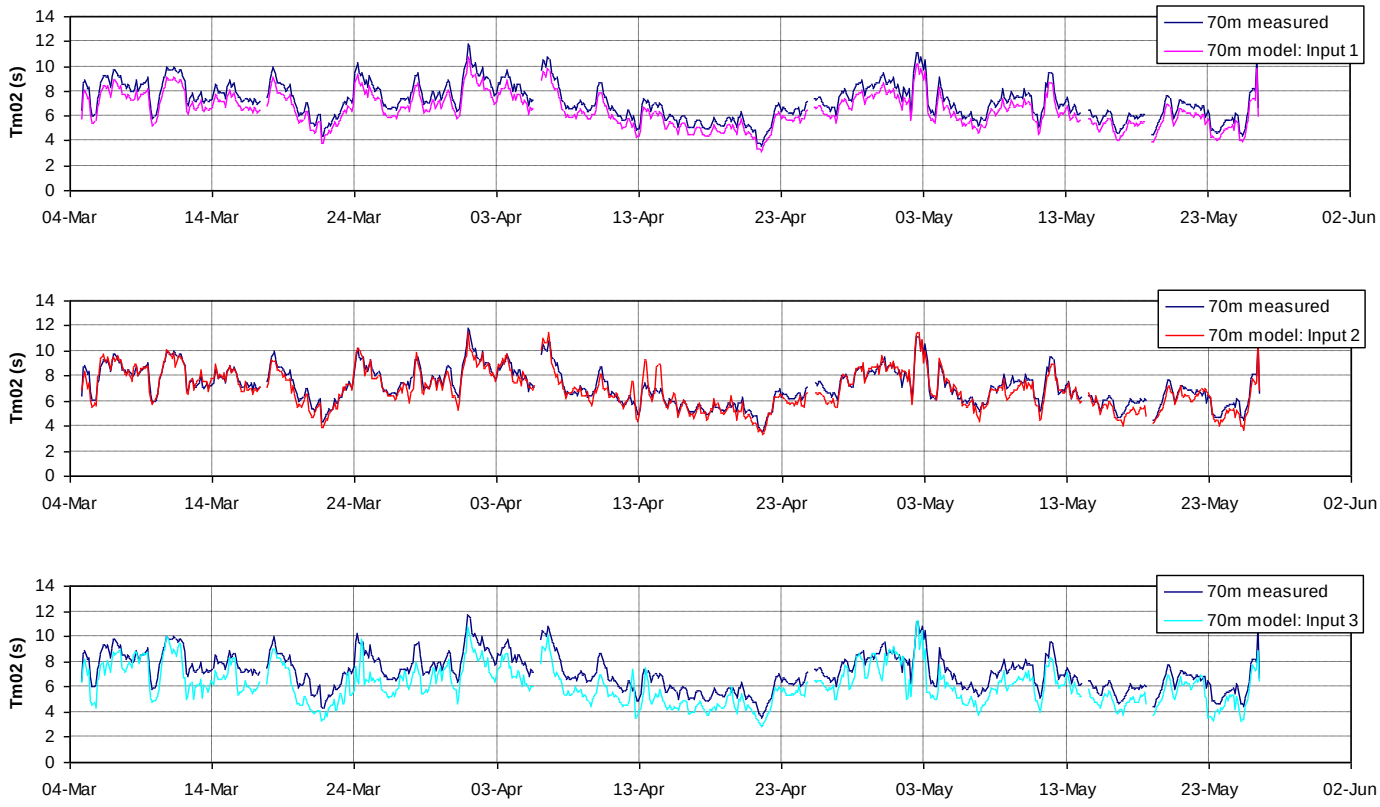

Figure 30 Time series comparison between modelled and recorded T_{m02} at the 70m buoy location for the three types of model input.

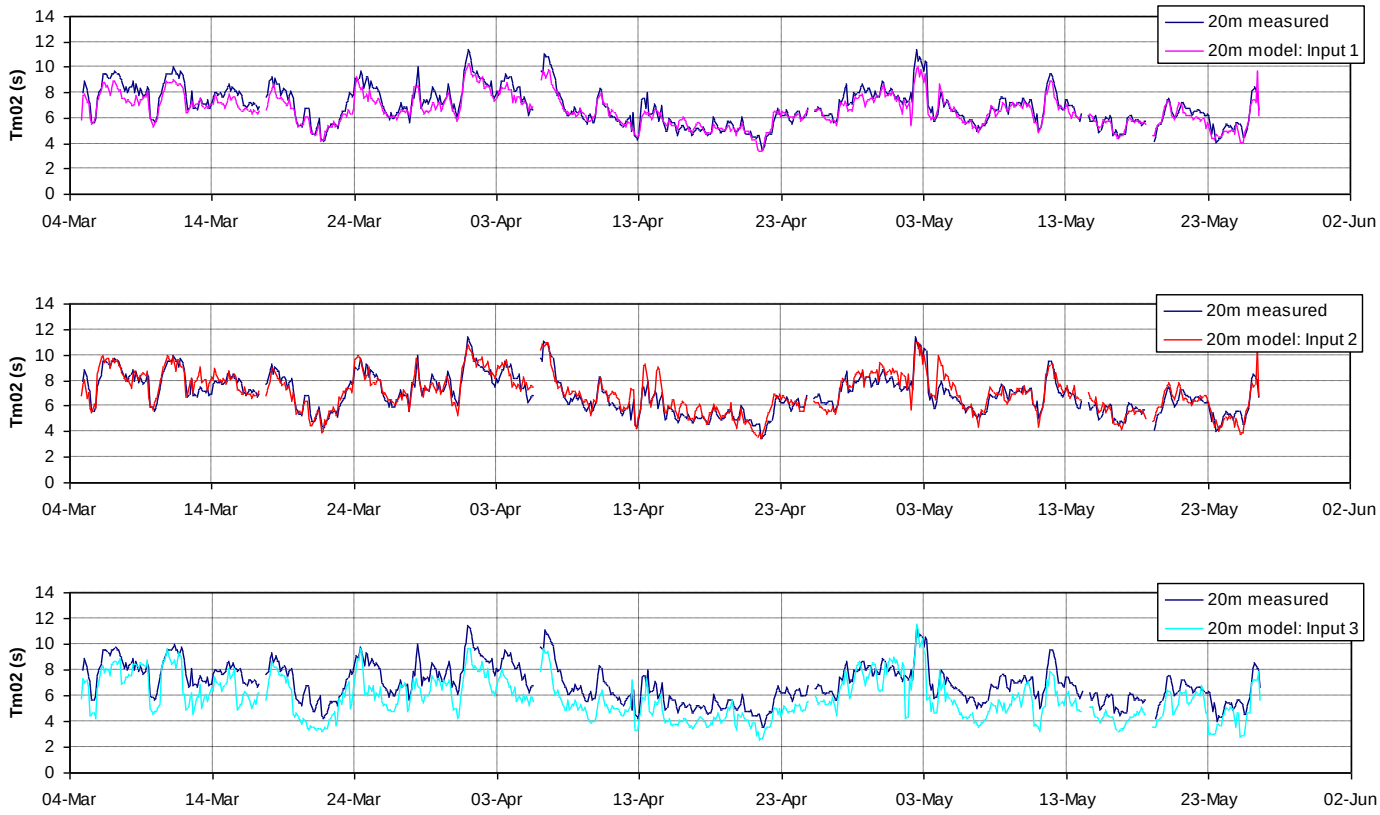

Figure 31 Time series comparison between modelled and recorded T_{m02} at the 20m buoy location for the three types of model input.

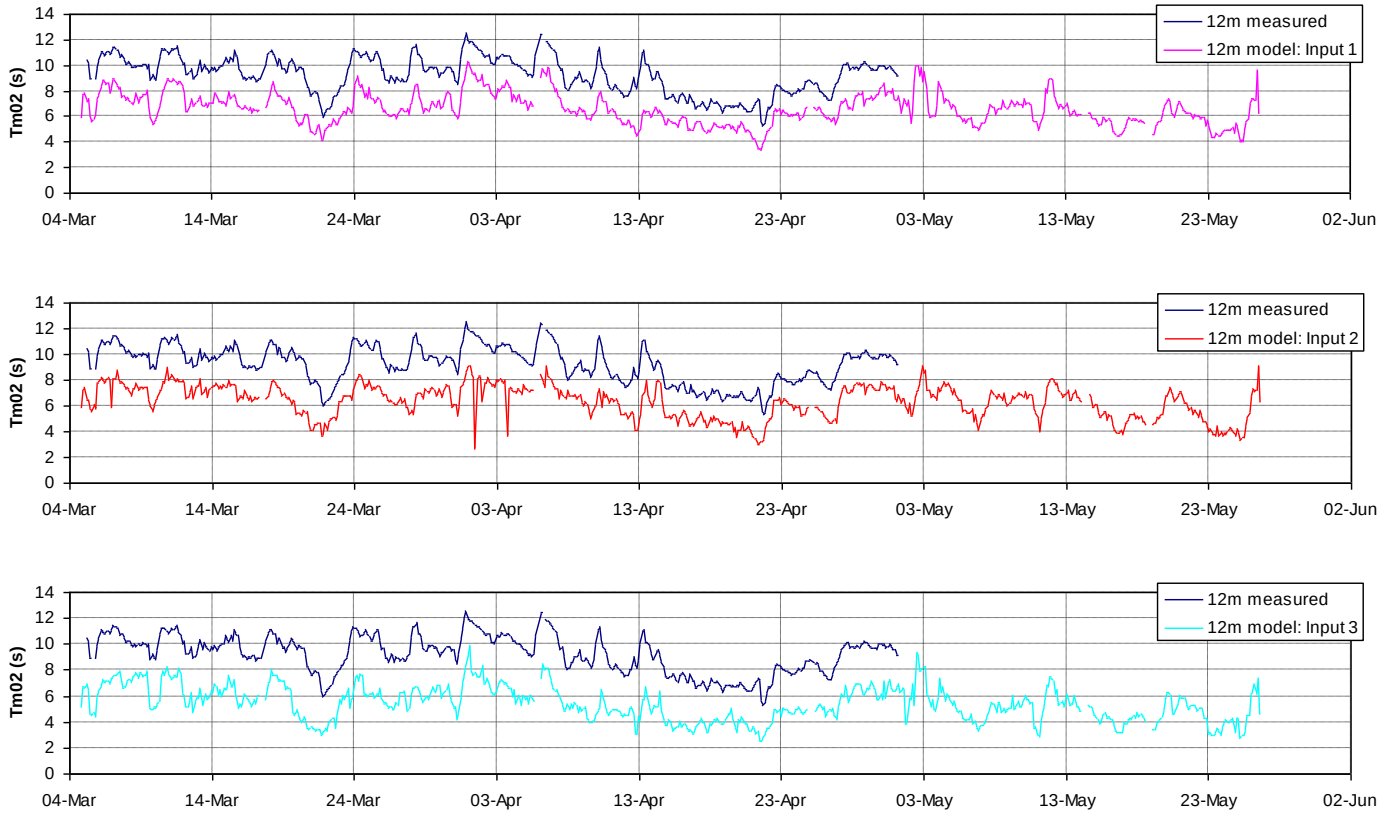

Figure 32 Time series comparison between modelled and recorded T_{m02} at the 12m buoy location for the three types of model input.

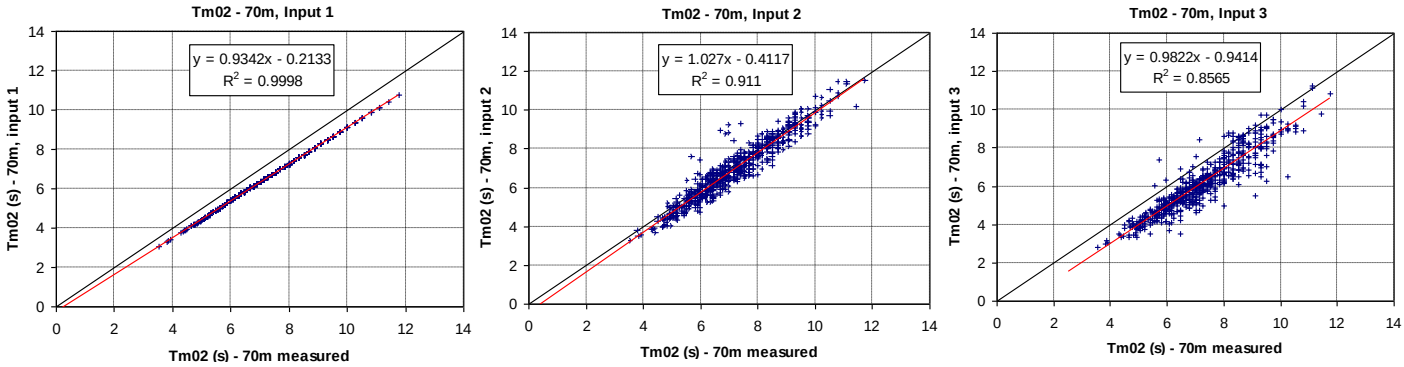

Figure 33 Scatter comparison between modelled and recorded T_{m02} at the 70m buoy location for the three types of model input.

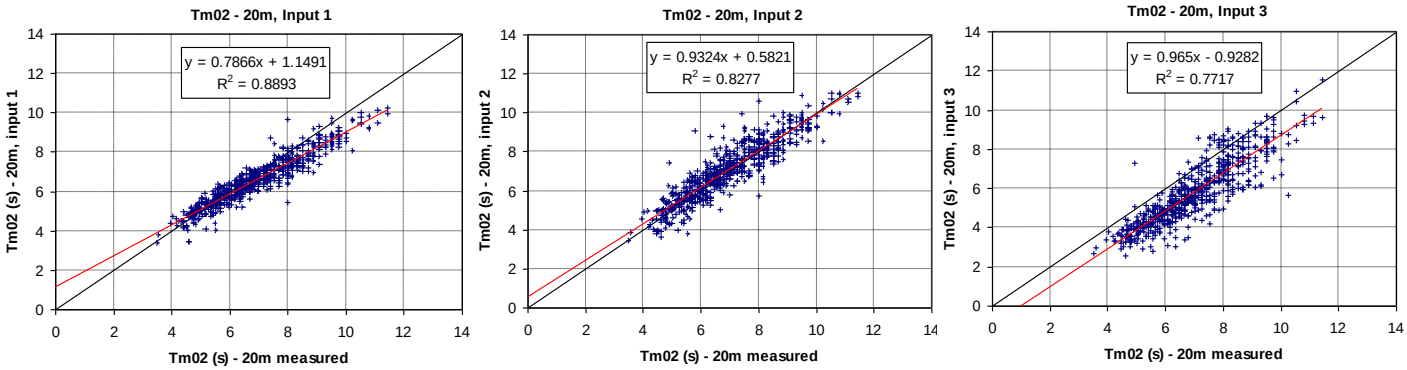

Figure 34 Scatter comparison between modelled and recorded T_{m02} at the 20m buoy location for the three types of model input.

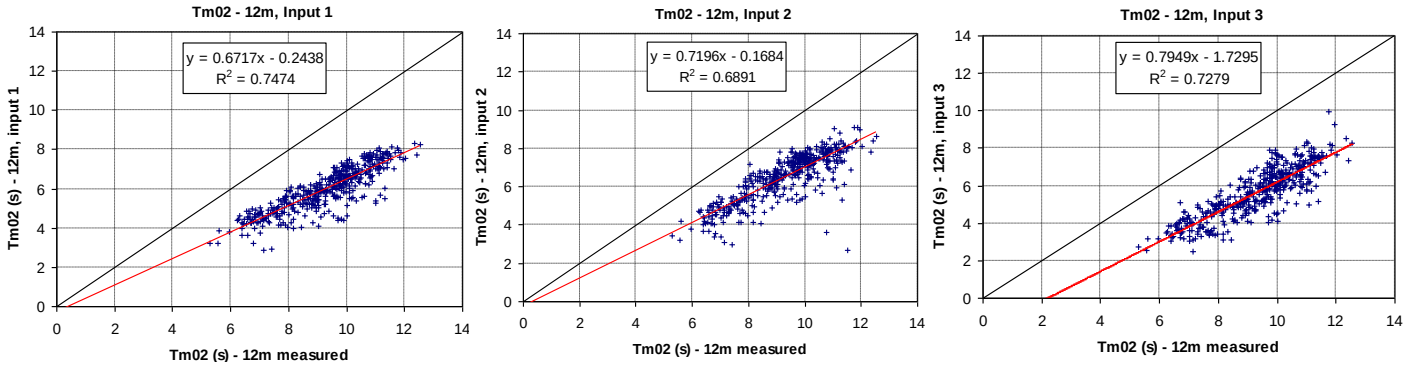

Figure 35 Scatter comparison between modelled and recorded T_{m02} at the 12m buoy location for the three types of model input.

Mean Direction

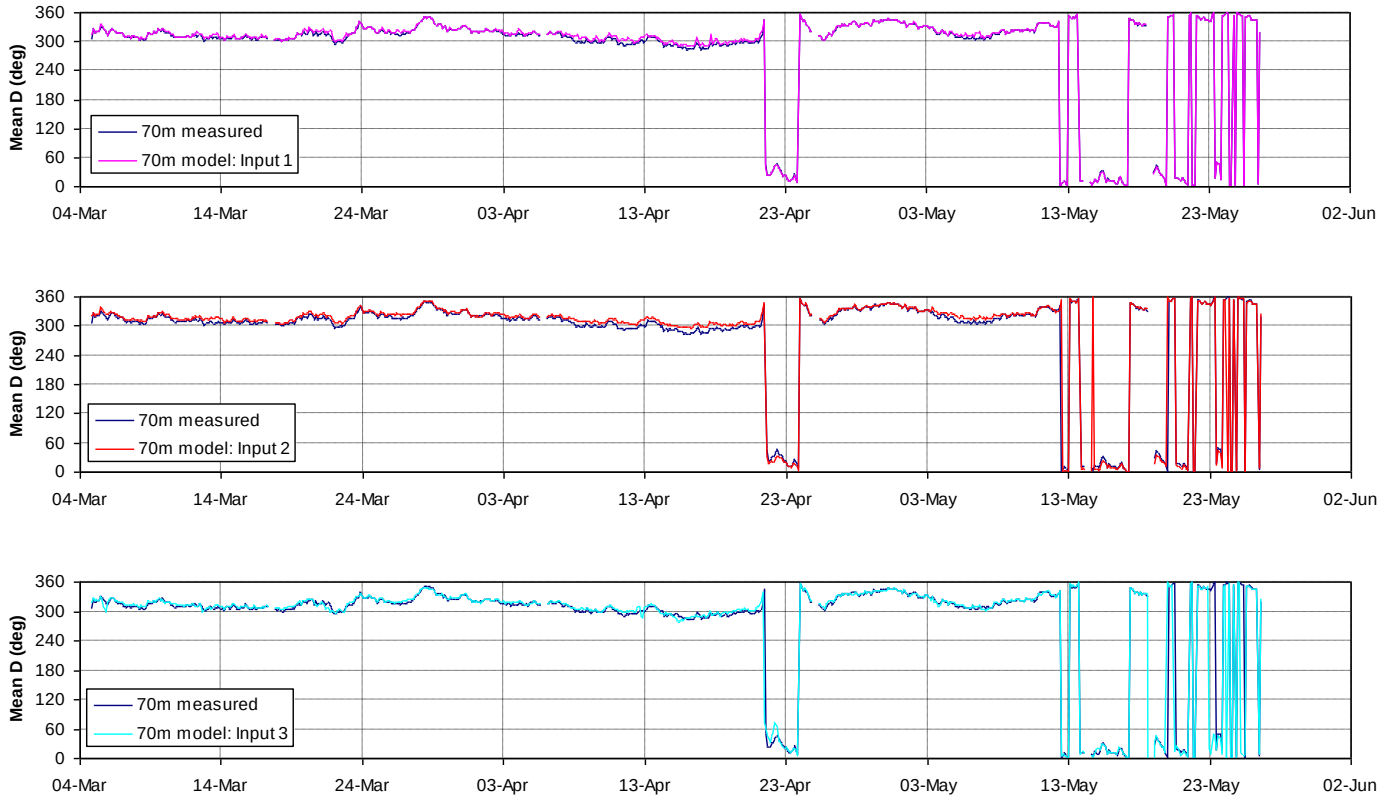

Figure 36 Time series comparison between modelled and recorded mean wave direction at the 70m buoy location for the three types of model input. Directions are measured anti-clockwise from East.

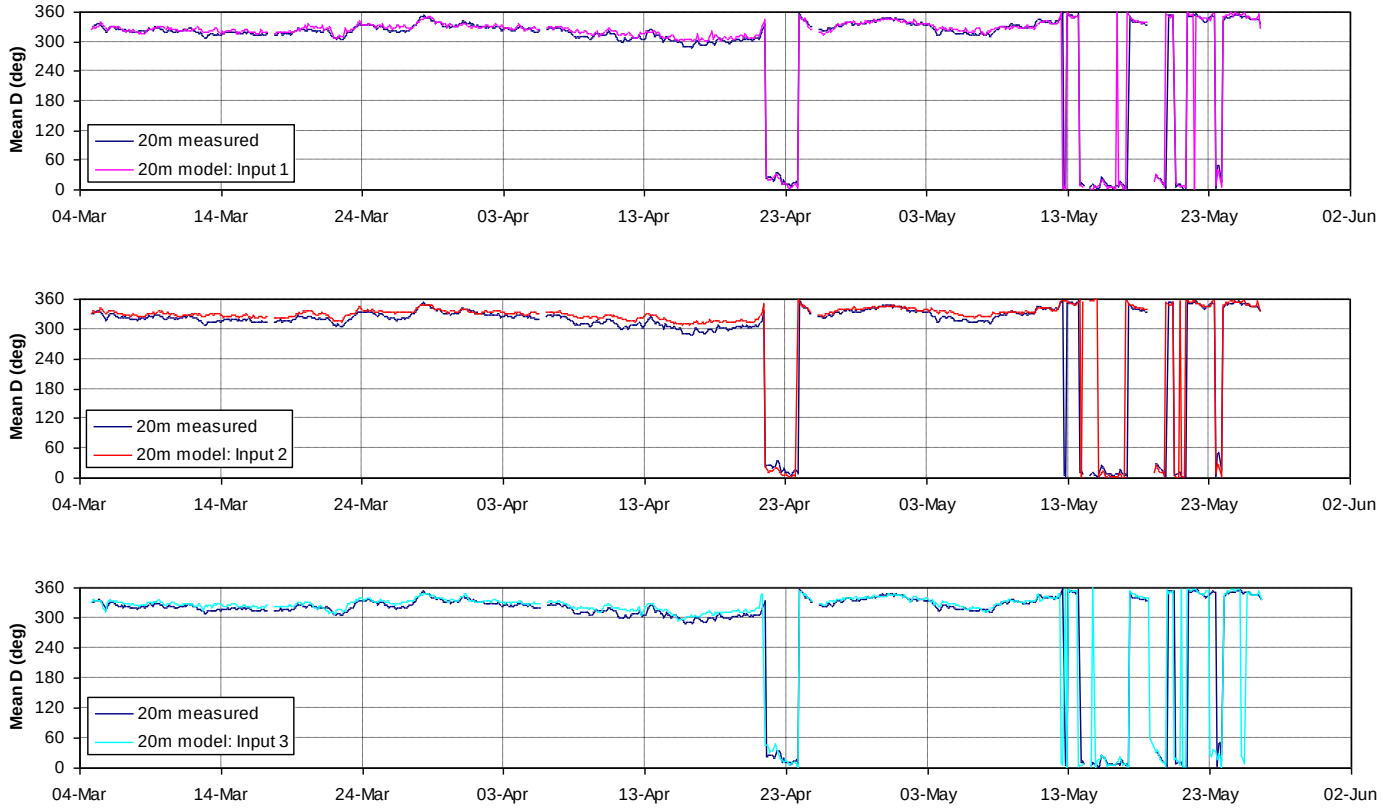

Figure 37 Time series comparison between modelled and recorded mean wave direction at the 20m buoy location for the three types of model input. Directions are measured anti-clockwise from East.

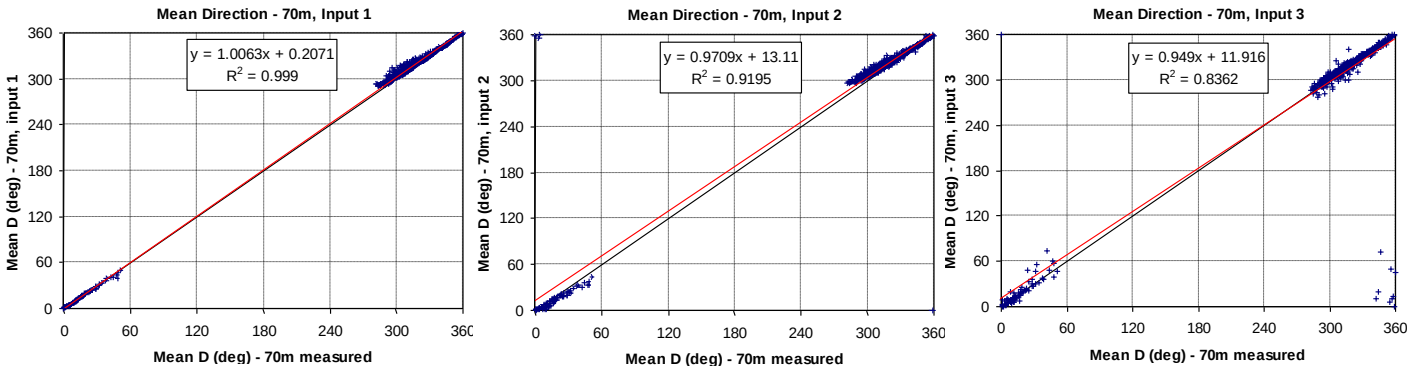

Figure 38 Scatter comparison between modelled and recorded mean wave direction at the 70m buoy location for the three types of model input. Directions are measured anti-clockwise from East.

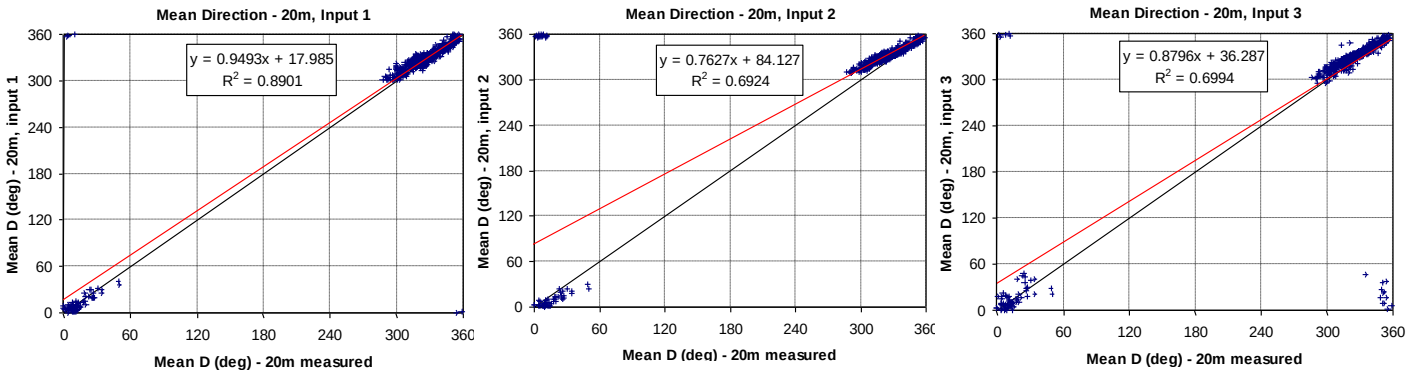

Figure 39 Scatter comparison between modelled and recorded mean wave direction at the 20m buoy location for the three types of model input. Directions are measured anti-clockwise from East.

3.5 TOMAWAC MODELLING

3.5.1 Model Setup

TOMAWAC is based on the use of unstructured finite element grid, hence the model setup is exactly the same that for SWAN modelling presented in §3.3. The computational mesh built for SWAN model was converted into the TELEMAC format. TOMAWAC was run with its default parameters.

3.5.2 Model Output

3.5.2.1 Significant wave height

The results of significant wave height from TOMAWAC wave model is presented in Figure 40 to Figure 43 for the Buoys DW2 and DW3. The measured significant wave height is indicated by the red coloured line and TOMAWAC model output significant wave height is by the blue line. As explained in §3.3.2.1, to improve the comparison on DW3 position (frequency sampling reduced to 0.5 Hz) the wave parameters (here H_{m0}) are also computed by considering a frequency cut-off of 0.24 Hz in the output spectra. These results are presented by the cyan coloured line on the temporal plots.

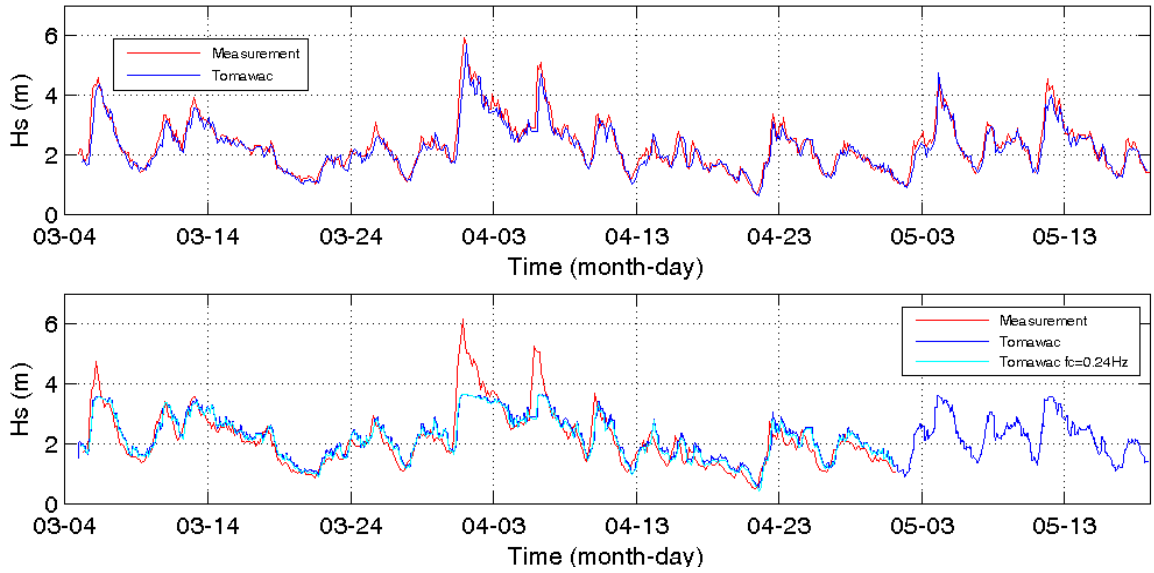

Figure 40 Significant wave height time series: (i) Buoy DW2 (20m water depth) – upper plot, and (ii) Buoy DW3 (12 m depth) – bottom plot. The wind forcing is not included in the modelling.

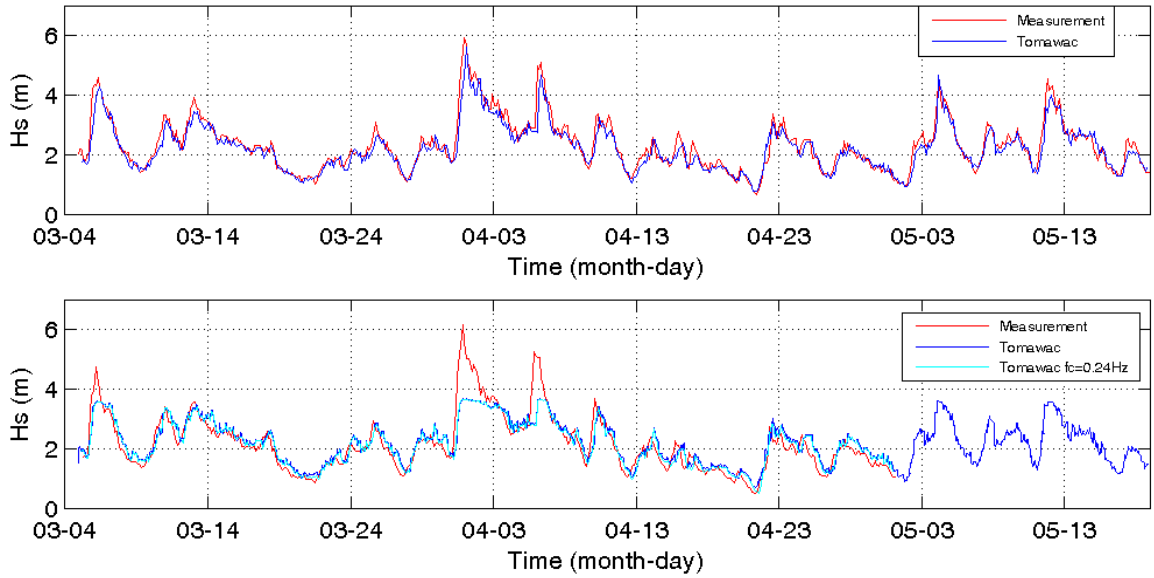

Figure 41 Significant wave height time series: (i) Buoy DW2 (20m water depth) – upper plot, and (ii) Buoy DW3 (12 m depth) – bottom plot. The wind forcing is included in the modelling.

The model output follows a similar trend as that of measurements. Similar to SWAN modelling, for the TOMAWAC computation both the 'wind forcing' and 'no wind forcing' cases have been simulated. The overall difference between the two cases is not significant as the fetch is short. On DW3 position, we note that highest events are largely underestimated.

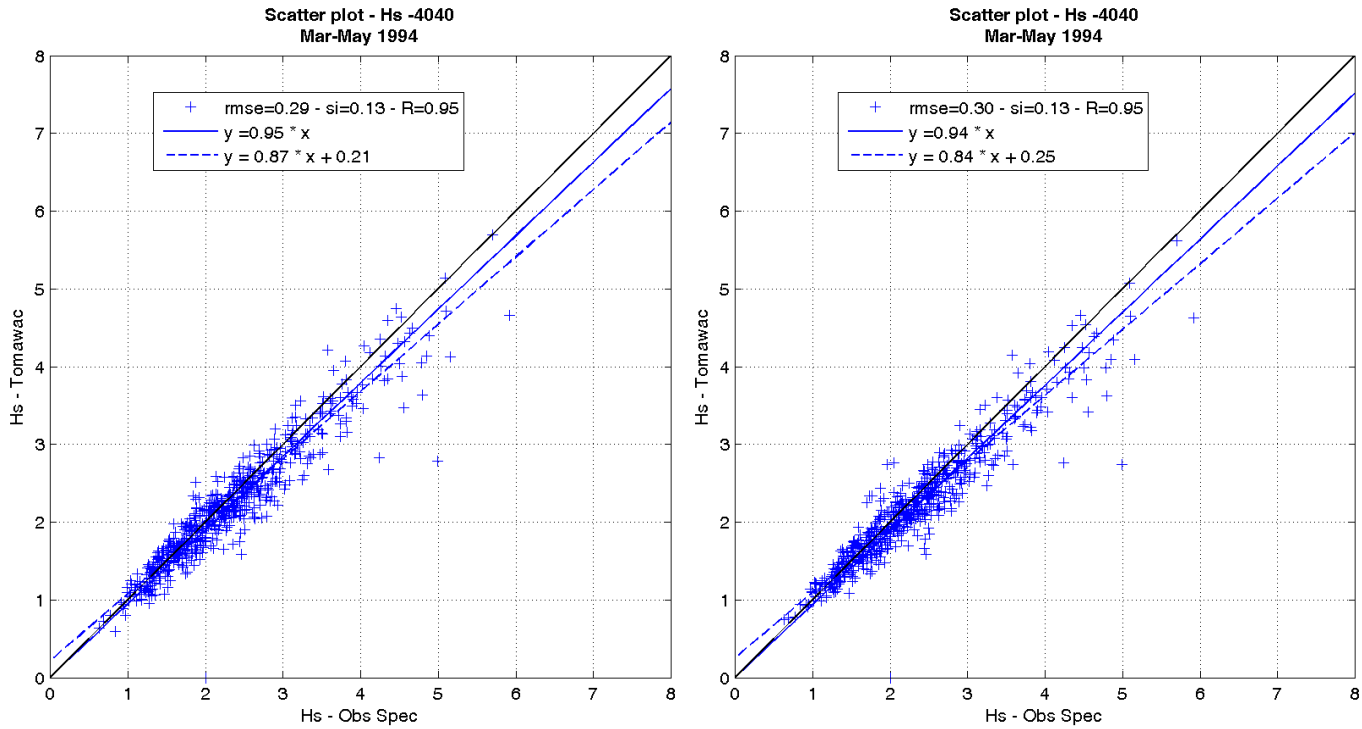

Figure 42 Comparison of Significant wave height between measurements and TOMAWAC for Buoy DW2: The left hand plot is for 'no wind' and the right hand plot is for 'wind input' included in the model.

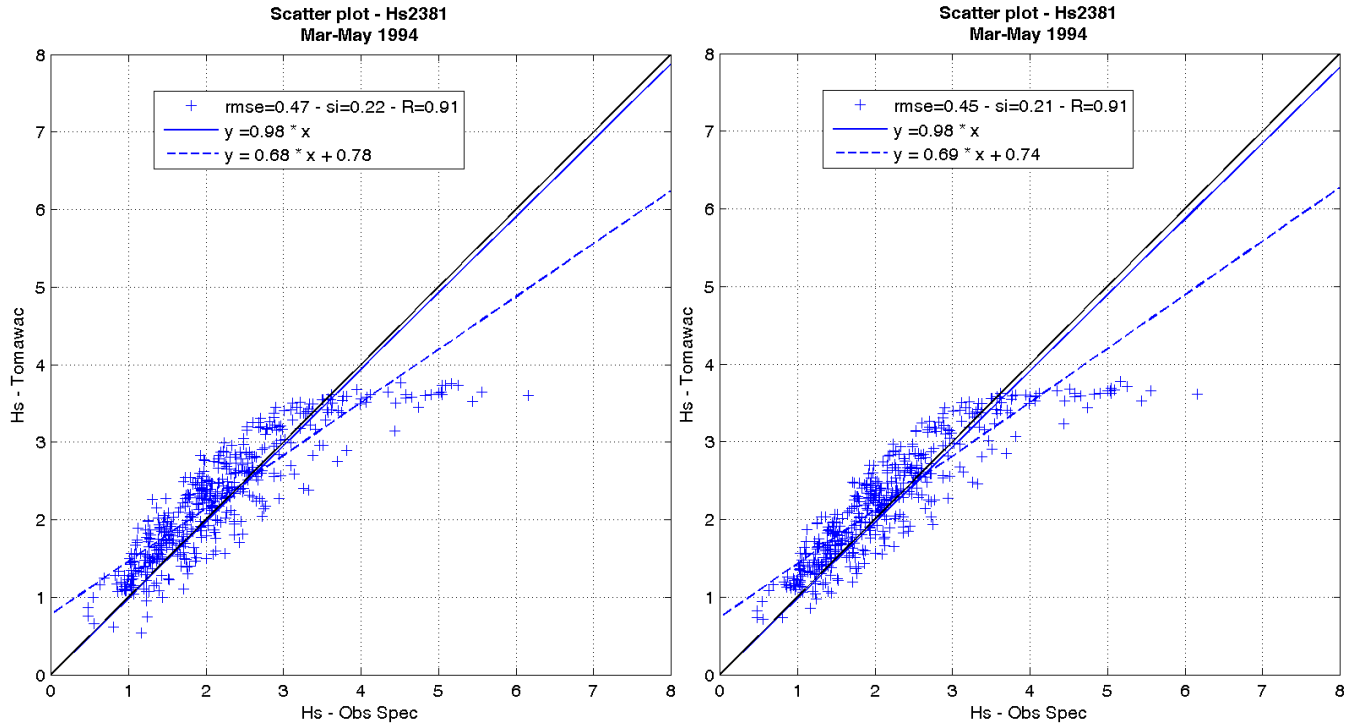

Figure 43 Comparison of Significant wave height between measurements and TOMAWAC for Buoy DW3: The left hand plot is for 'no wind' and the right hand plot is for 'wind input' included in the model.

3.5.2.2 Mean wave direction

The mean wave direction obtained using TOMAWAC model is compared in Figure 44 to Figure 46. As expected excellent correlation exists between measured and simulated mean wave directions with R = 0.97.

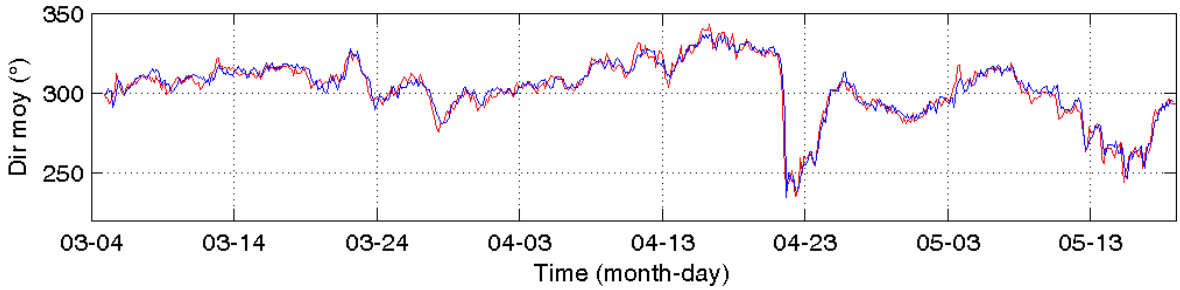

Figure 44 Time series of Mean wave direction: Buoy DW2 (20m water depth) – bottom plot. The wind forcing is not included in the modelling. Measurement -red, TOMAWAC – blue.

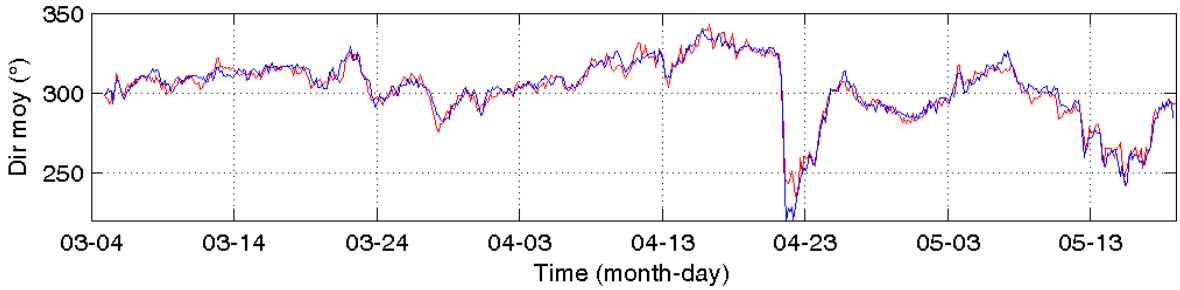

Figure 45 Time series of Mean wave direction: Buoy DW2 (20m water depth) – bottom plot. The wind forcing is included in the modelling. Measurement -red, TOMAWAC – blue.

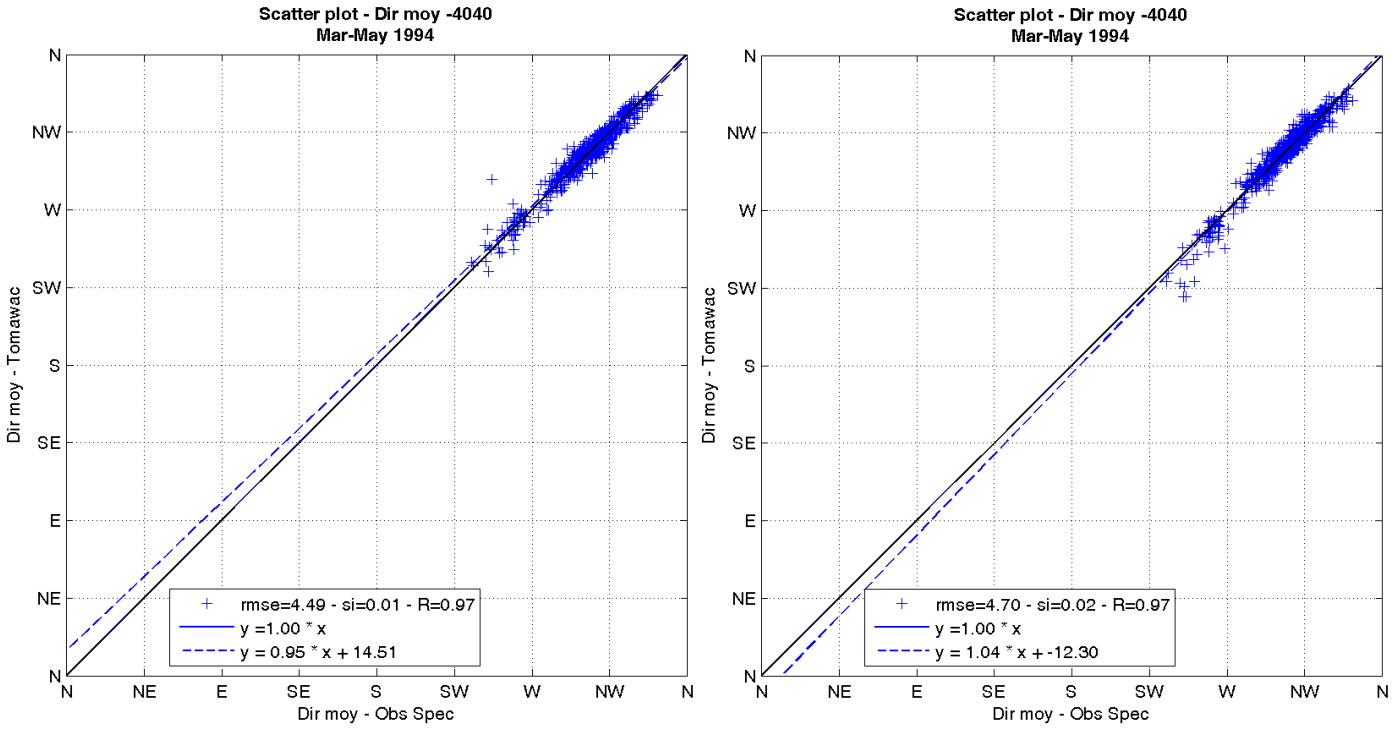

Figure 46 Comparison of Mean wave direction between measurements and TOMAWAC model for Buoy DW2: The left hand plot is for 'no wind' and the right hand plot is for 'wind input' included in the model.

3.5.2.3 Wave Periods (Tp and Tm02)

The peak wave period (T_p) and mean wave period (T_{m02}) from the measurements and TOMAWAC model are shown in Figure 47 to Figure 52. On the temporal plots, measurement is indicated by the red coloured line and TOMAWAC standard output is by the blue line. On DW3 position, the T_{m02} is also computed by considering a frequency cut-off of 0.24 Hz in the output spectra. These results are presented by the cyan coloured line on the temporal plots.

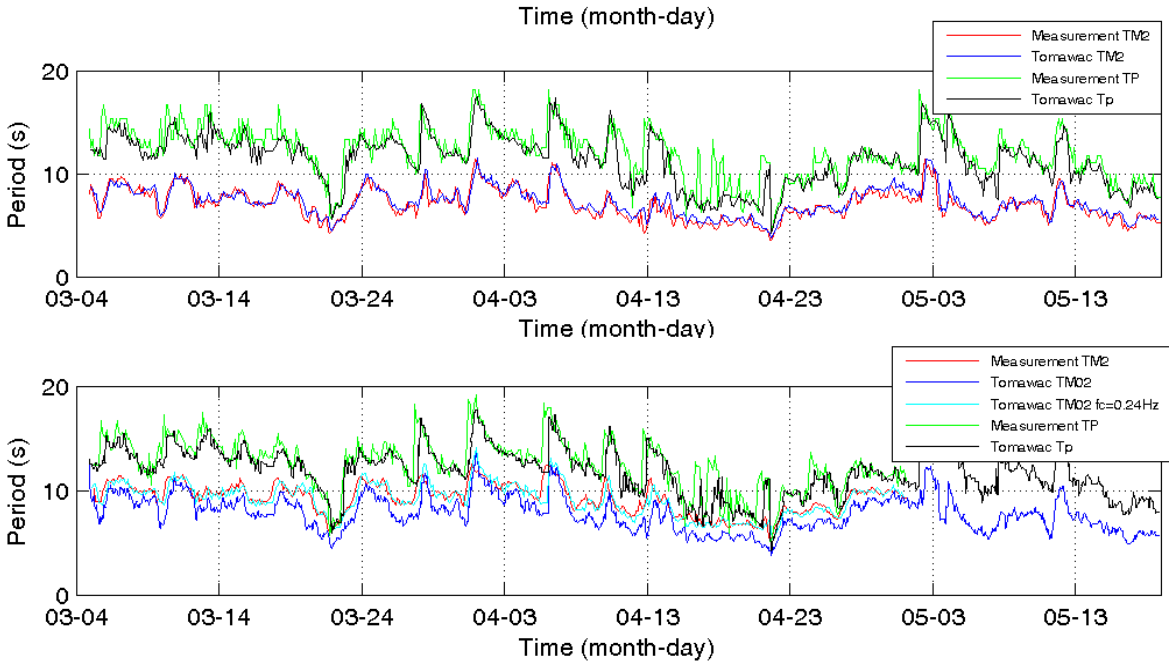

Figure 47 Zero crossing wave period (T_{m02}) and peak wave period (T_p) time series: (i) Buoy DW2 (20m water depth) – middle plot, and (iii)) Buoy DW3 (12 m depth) – bottom plot. The wind forcing is not included in the modelling.

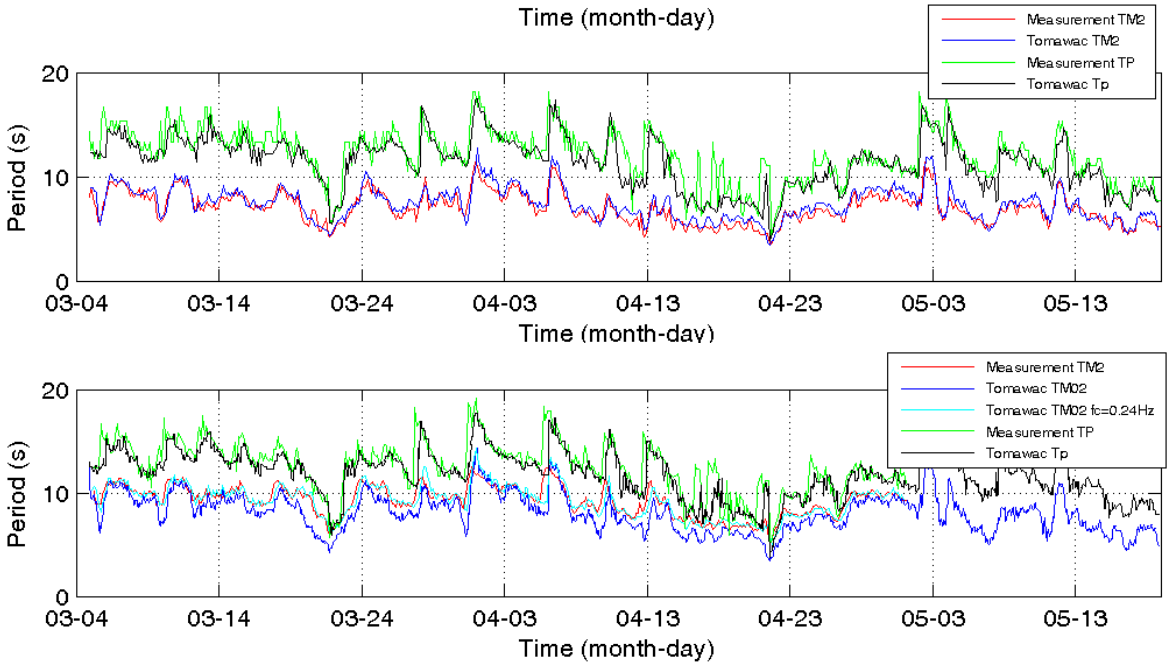

Figure 48 Zero crossing wave period (T_{m02}) and peak wave period (T_p) time series: (i) Buoy DW2 (20m water depth) – middle plot, and (iii)) Buoy DW3 (12 m depth) – bottom plot. The wind forcing is included in the modelling.

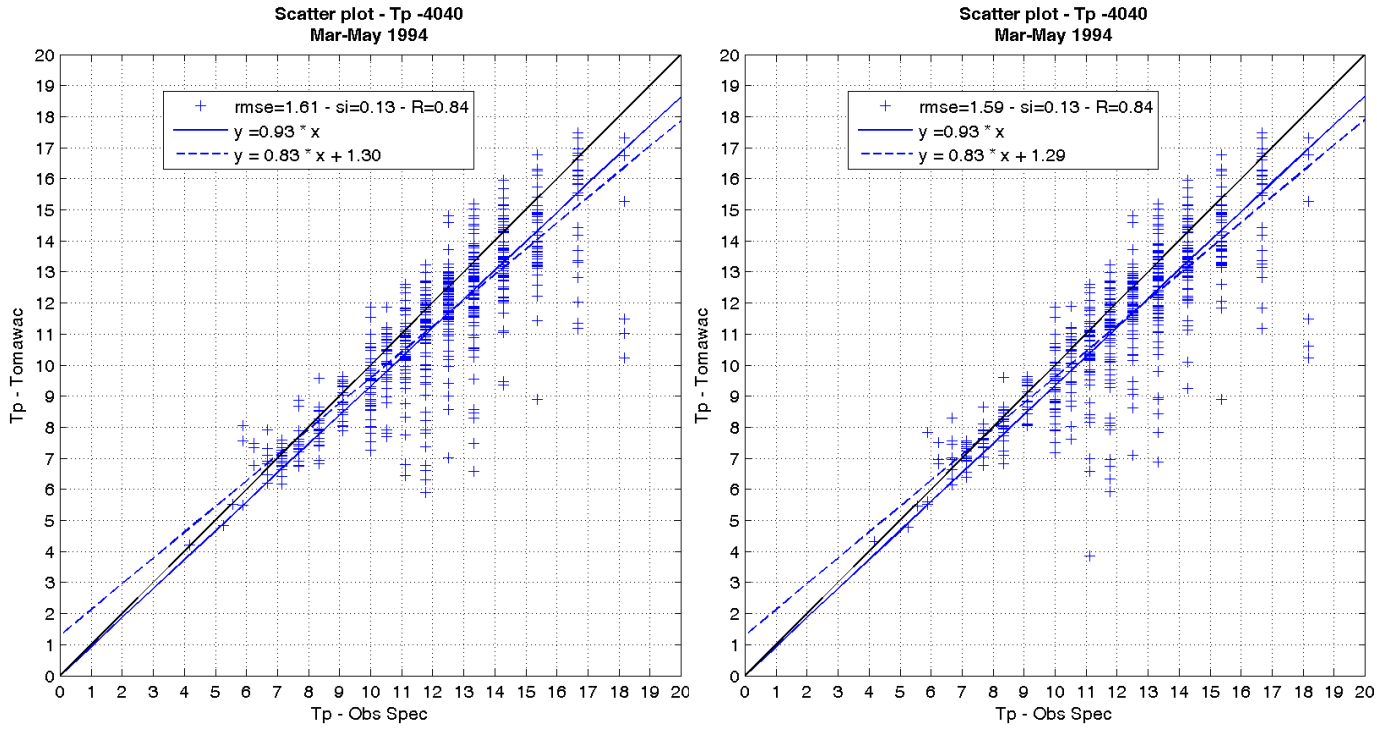

Figure 49 Comparison of peak wave period (T_p) between measurements and TOMAWAC model for Buoy DW2: The left hand plot is for 'no wind' and the right hand plot is for 'wind input' included in the model.

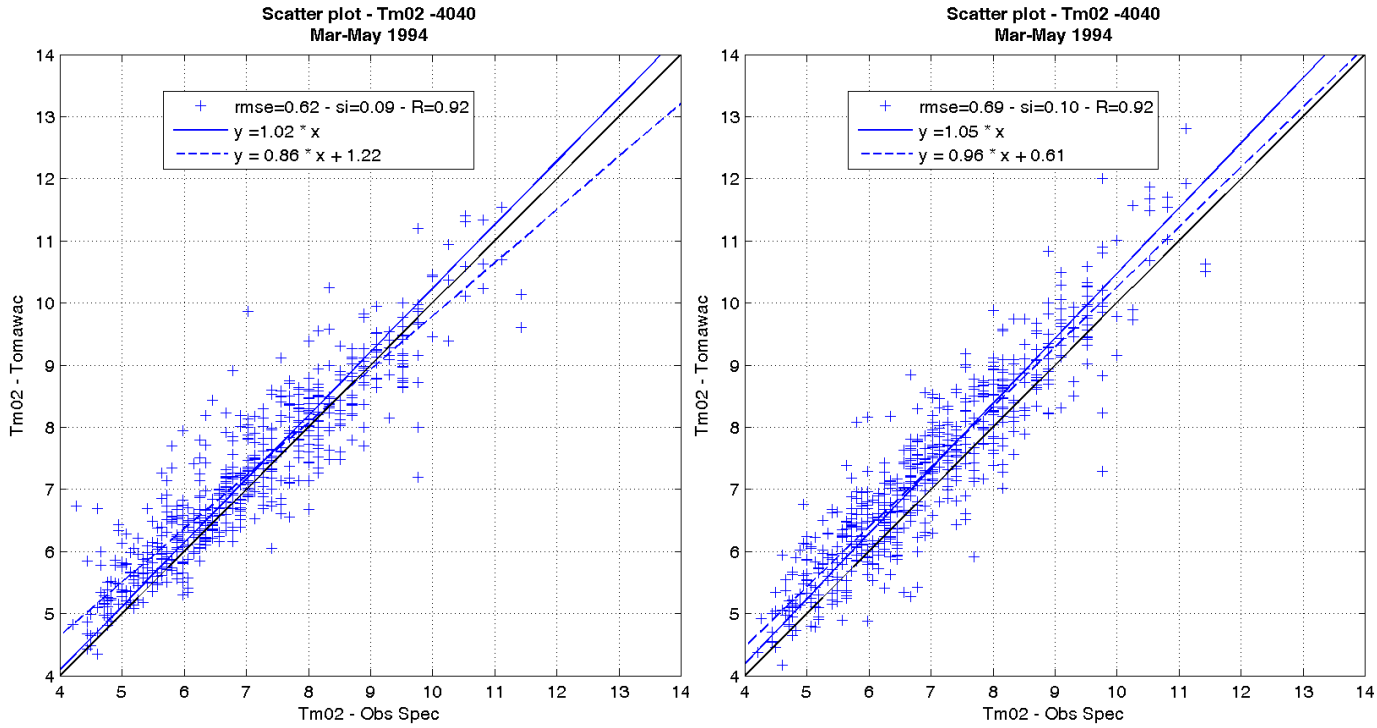

Figure 50 Comparison of zero crossing wave period (T_{m02}) between measurements and TOMAWAC model for Buoy DW2: The left hand plot is for 'no wind' and the right hand plot is for 'wind input' included in the model.

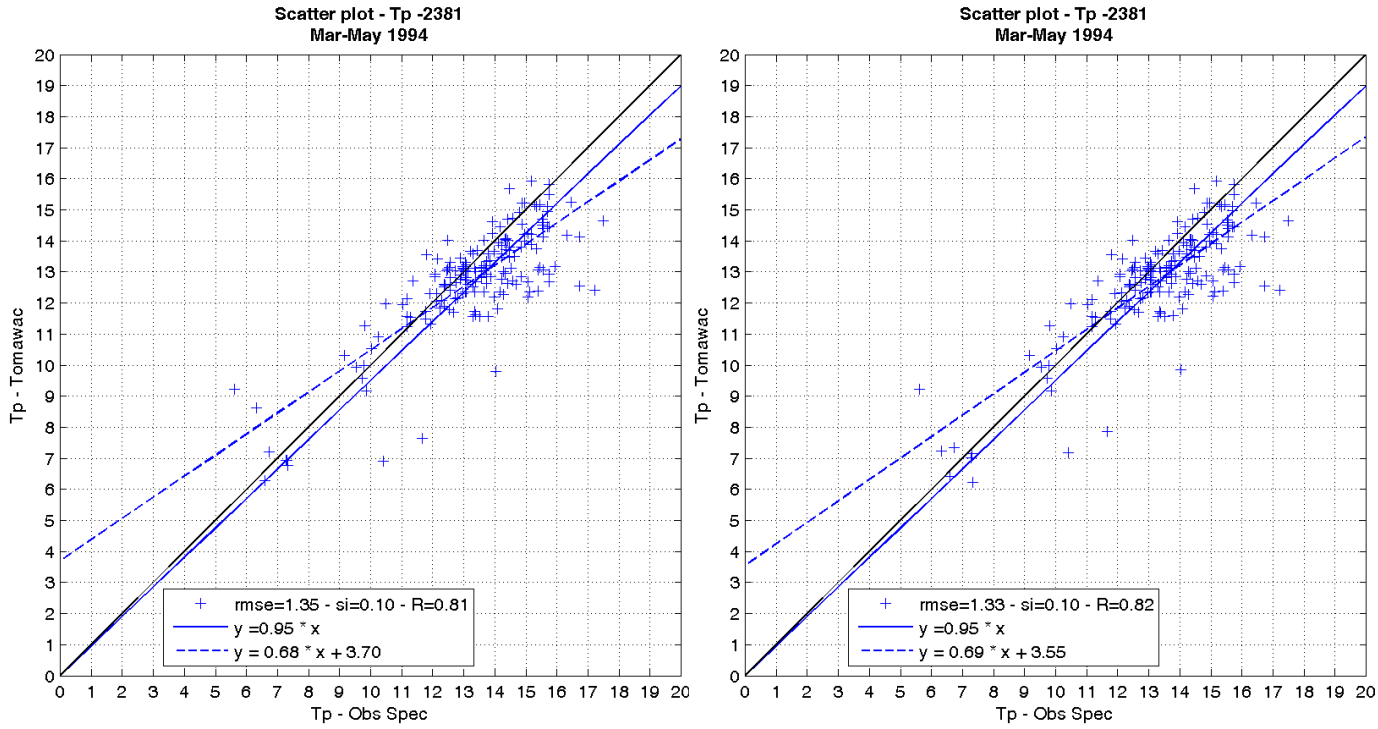

Figure 51 Comparison of peak wave period (T_p) between measurements and TOMAWAC model for Buoy DW3: The left hand plot is for 'no wind' and the right hand plot is for 'wind input' included in the model.

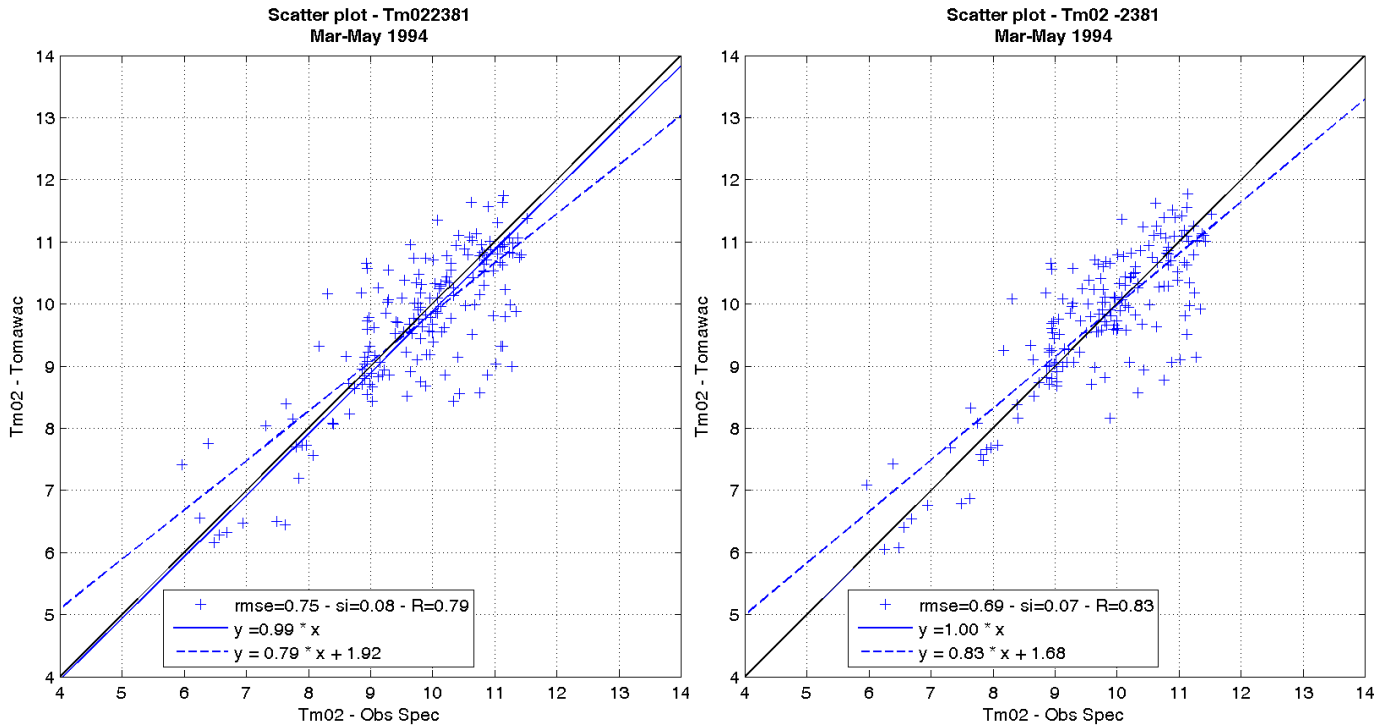

Figure 52 Comparison of zero crossing wave period (T_{m02}) between measurements and TOMAWAC model for Buoy DW3: The left hand plot is for 'no wind' and the right hand plot is for 'wind input' included in the model.

3.6 MIKE21 MODELLING

3.6.1 Model Setup

An unstructured computational mesh was used for the MIKE21 wave modelling. The bathymetry generated with the C-Map (Figure 5) has been used with MIKE21 model. The computational mesh information is given below.

Number of elements : 479
Number of faces : 763
Number of nodes : 285
Number of sections : 5
Min x-coordinate : 483364
Max x-coordinate : 519815
Min y-coordinate : 4413440
Max y-coordinate : 4497570
Min z-coordinate : -92.819032
Max z-coordinate : 0

The number of directions used were 18 and the number of frequencies used were 25 with f_{min} = 0.04 Hz. The frequency factor was 1.1 and a logarithmic distribution of frequencies was generated. The directionally decoupled spectral formulation with quasi stationary time formulation was used. No current, wind, ice coverage and diffraction were used. Dissipation due to whitecapping, bottom friction and depth-induced wave breaking were considered in the simulations and the energy transfer was activated

3.6.2 Model Output

3.6.2.1 Significant wave height

The significant wave height and peak wave period obtained from MIKE21 simulations are shown in Figure 53 and Figure 54 respectively, at 05/04/1994, 00:57:59. The variation of wave height and periods over the domain, and the wave transformation from deep water to coastal areas can be clearly seen in these plots. The time series of significant wave height extracted at the locations of buoy DW1 at 70m, buoy DW2 at 20m and buoy DW3 at 12m are plotted with measured data in Figure 55. The relationship between measurement and model results are correlated in Figure 56. The correlation coefficient is presented as R^2 value for MIKE21 modelling. A high R^2 value (= 0.99) can be seen for DW3 which is expected. Similarly a high correlation with R^2 = 0.956 (i.e., R = 0.978) is observed for 20m depth. At 12m depth, similar to SWAN and TOMAWAC models, MIKE21 also produced a smaller R^2 = 0.891(i.e., R = 0.944).

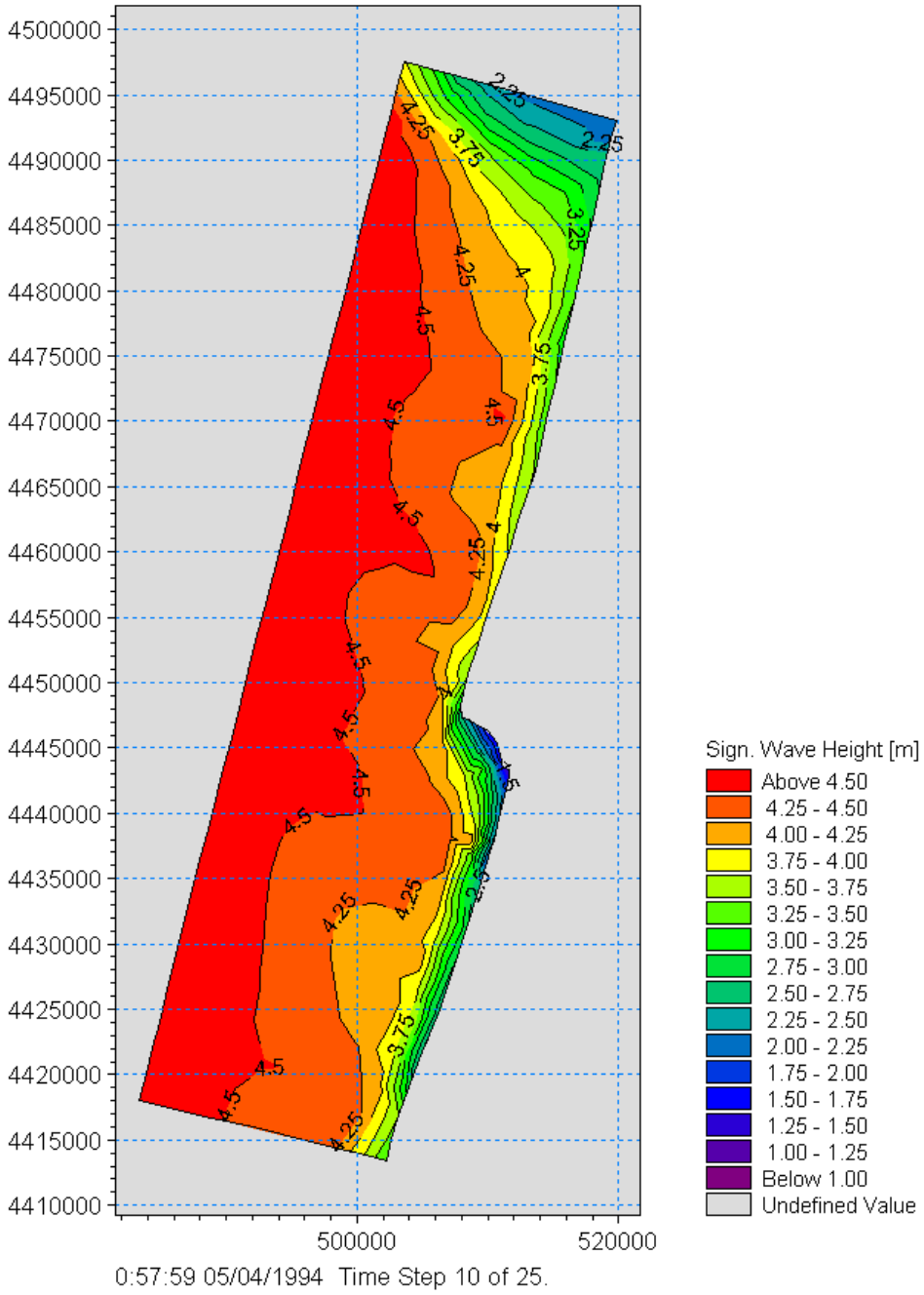

Figure 53 Spatial variation of significant wave height over the computational domain

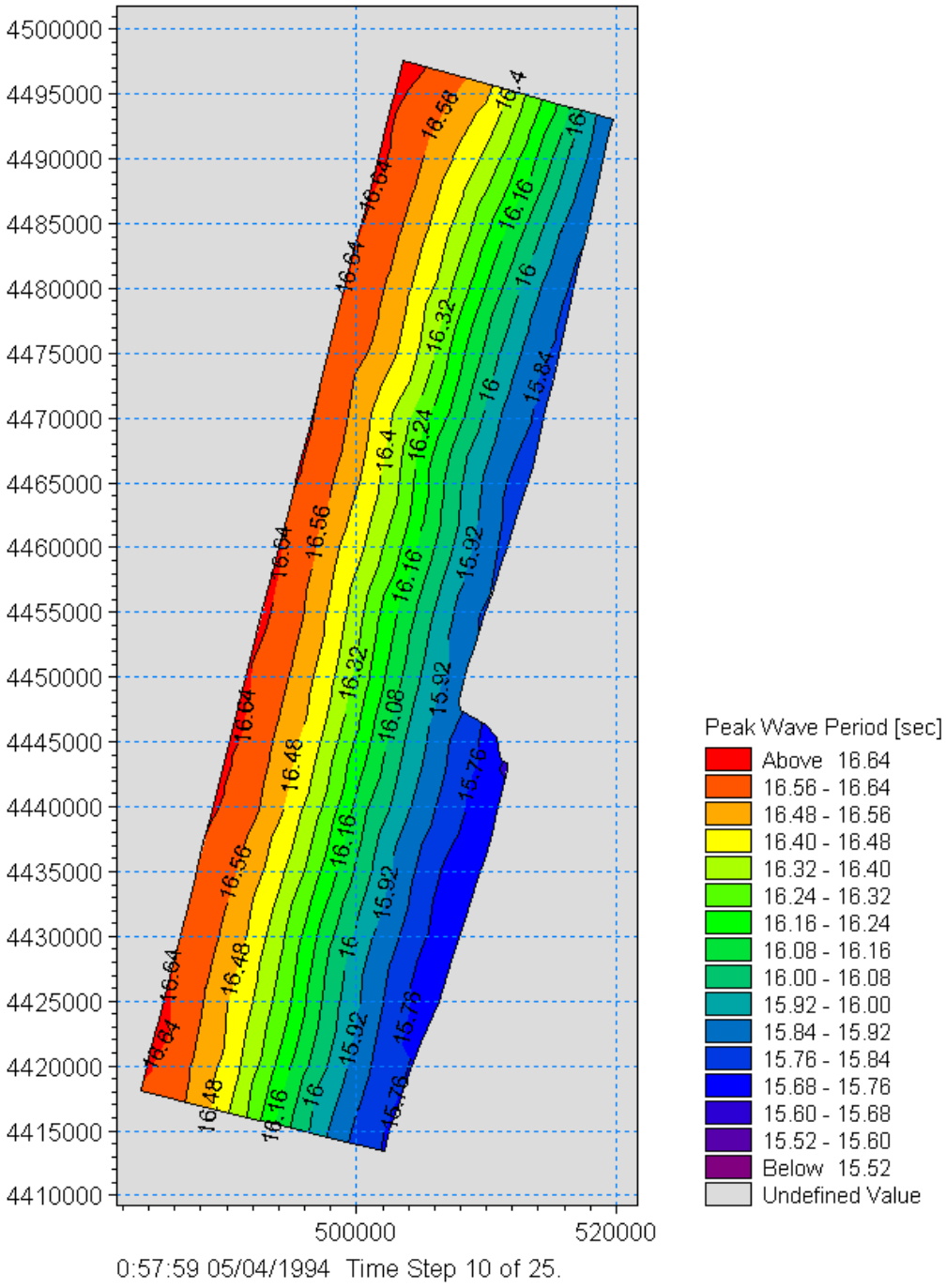

Figure 54 Spatial variation of peak wave period over the computational domain

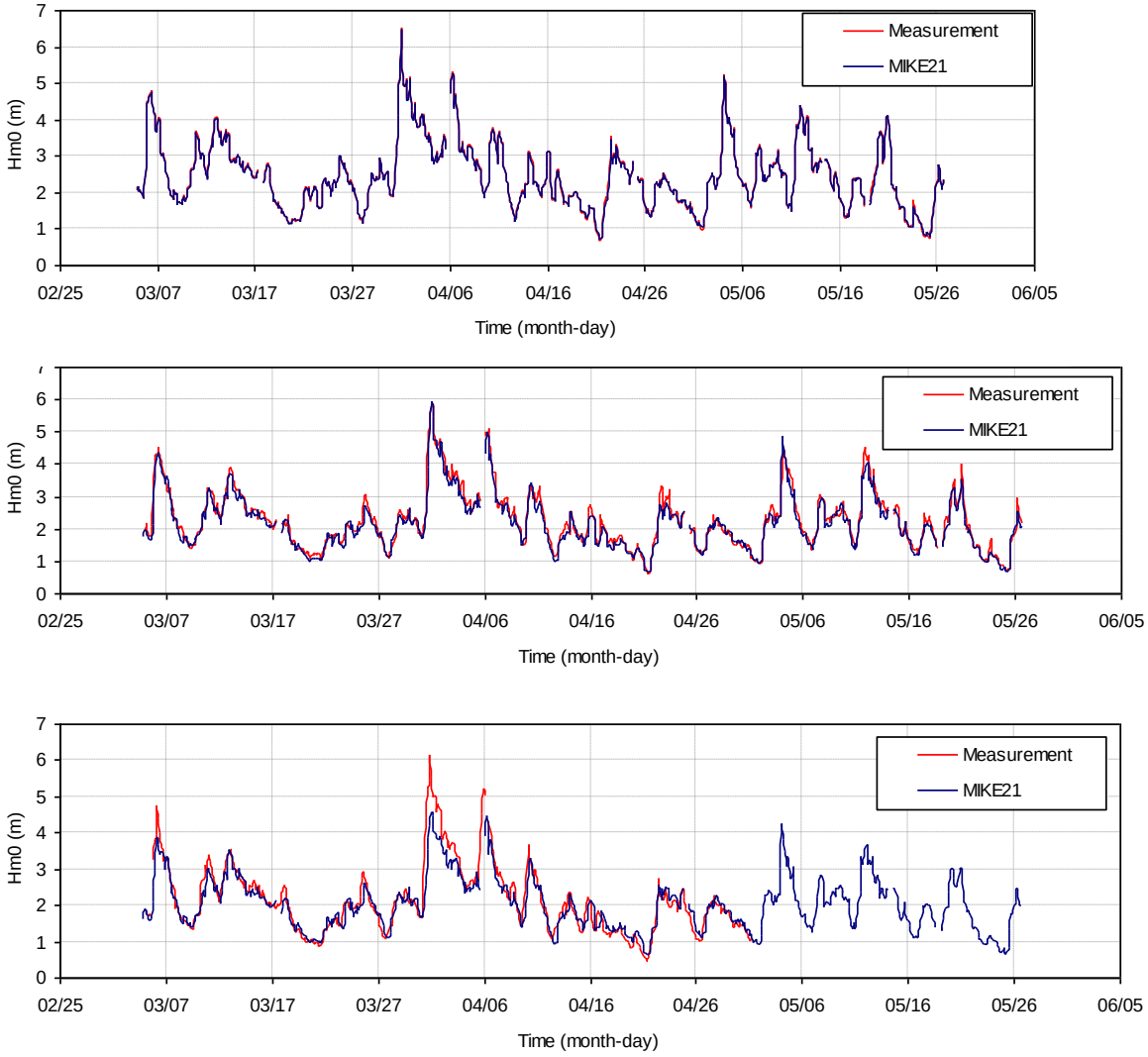

Figure 55 Significant wave height time series: (i) Buoy DW1 offshore buoy (at 70m depth) – upper plot, (ii) Buoy DW2 (20m water depth) – middle plot, and (iii)) Buoy DW3 (12 m depth) – bottom plot. The wind forcing is not included in the modelling

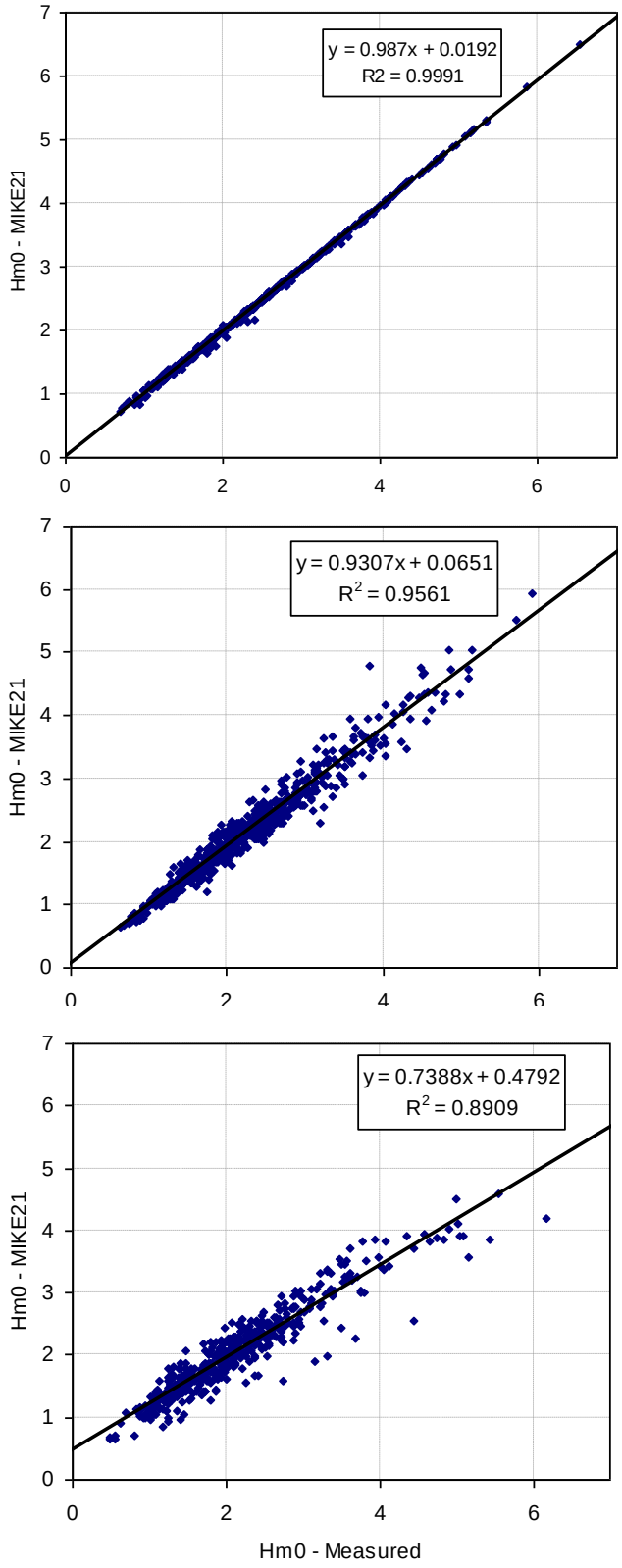

Figure 56 Comparison of Significant wave height between measurements and MIKE21 model: (i) Buoy DW1 offshore buoy (at 70m depth) – upper plot, (ii) Buoy DW2 (20m water depth) – middle plot, and (iii) Buoy DW3 (12 m depth) – bottom plot. The wind forcing is not included in the modelling.

3.6.2.2 Mean wave direction

Time series plots of measured mean wave direction and MIKE21 output are shown in Figure 57 for depths 70m and 20m. The scatter plots showing correlation between these quantities are illustrated in Figure 58. In general the comparison is excellent. For the buoy DW2 a high R^2 value (i.e., R = 0.966) is observed.

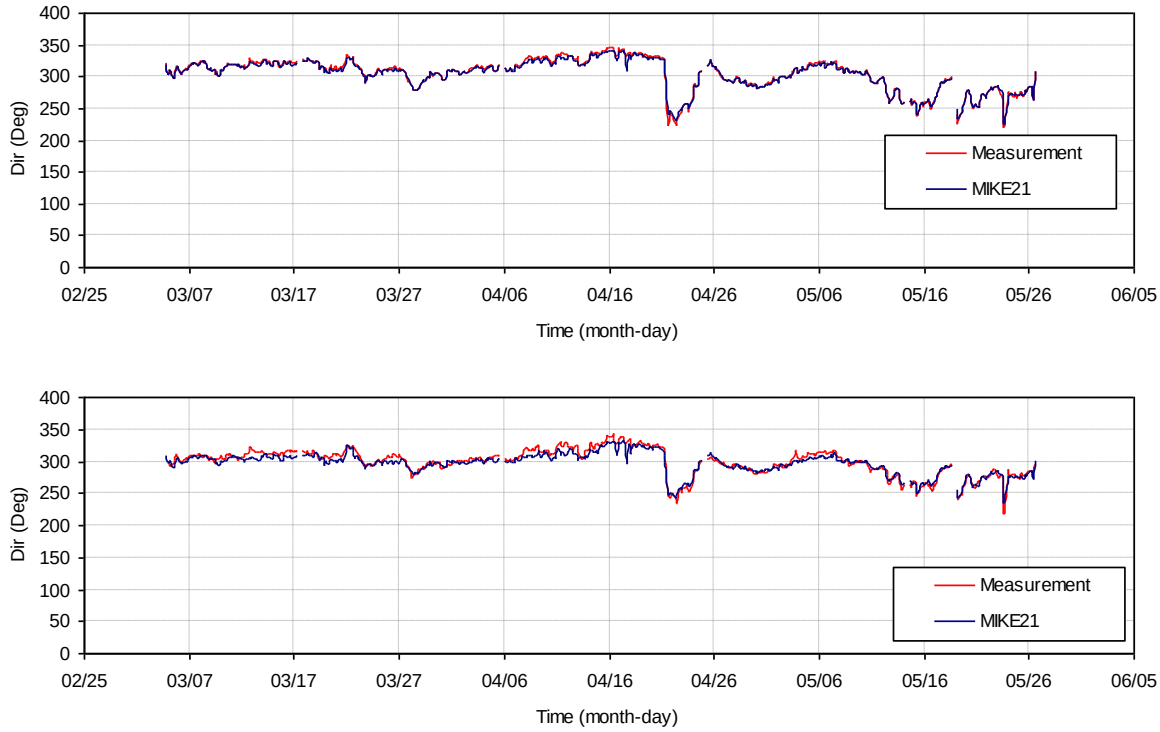

Figure 57 Time series of Mean wave direction: (i) Buoy DW1 offshore buoy (at 70m depth) – upper plot, (ii)) Buoy DW2 (20m water depth) – bottom plot. The wind forcing is not included in the modelling. Measurement -red, MIKE21 modelling – blue

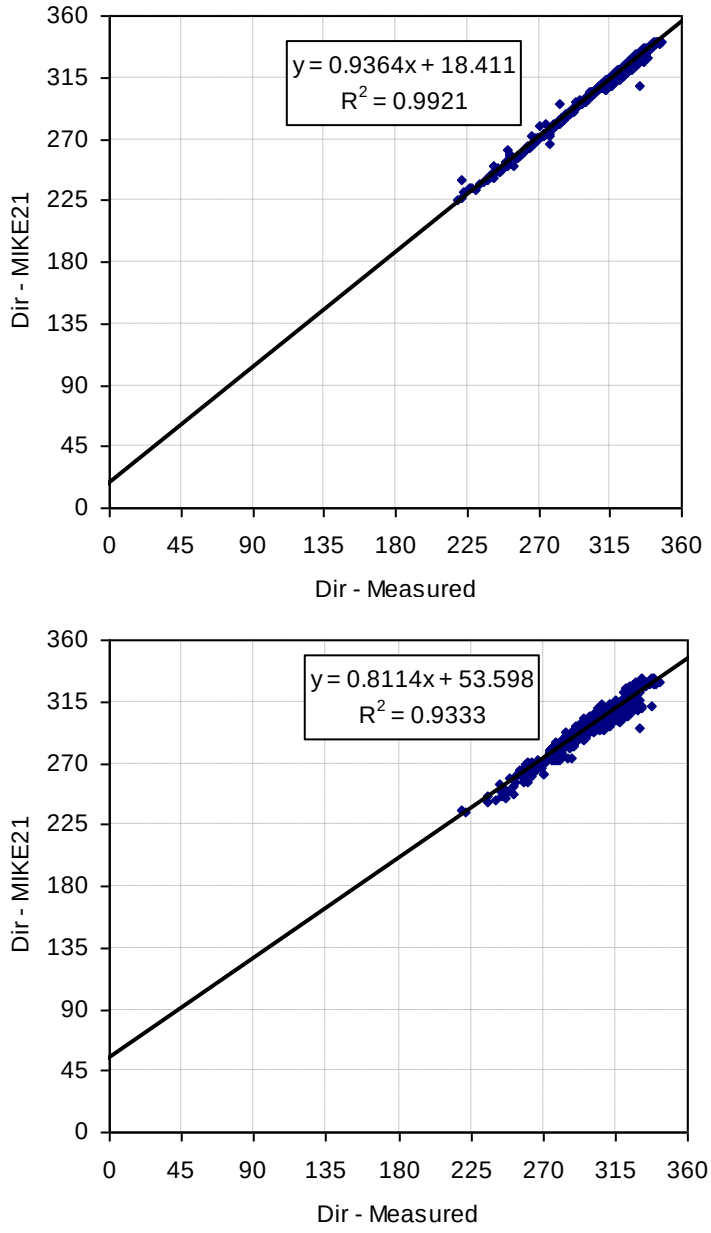

Figure 58 Comparison of mean wave direction between measurements and MIKE21 model: (i) Buoy DW1 offshore buoy (at 70m depth) – upper plot, (ii) Buoy DW2 (20m water depth) – bottom plot. The wind forcing is not included in the modelling

3.6.2.3 Wave Periods (Tp)

The peak wave period calculated from MIKE21 model is plotted with measurements at different water depths in Figure 59 and correlation plots in Figure 60. It is clear from these plots that the peak wave period has a high degree of scatter for depths 20m (R^2 = 0.7393, i.e., R = 0.86) and 12m (R^2 = 0.6278, i.e., R =0.792).

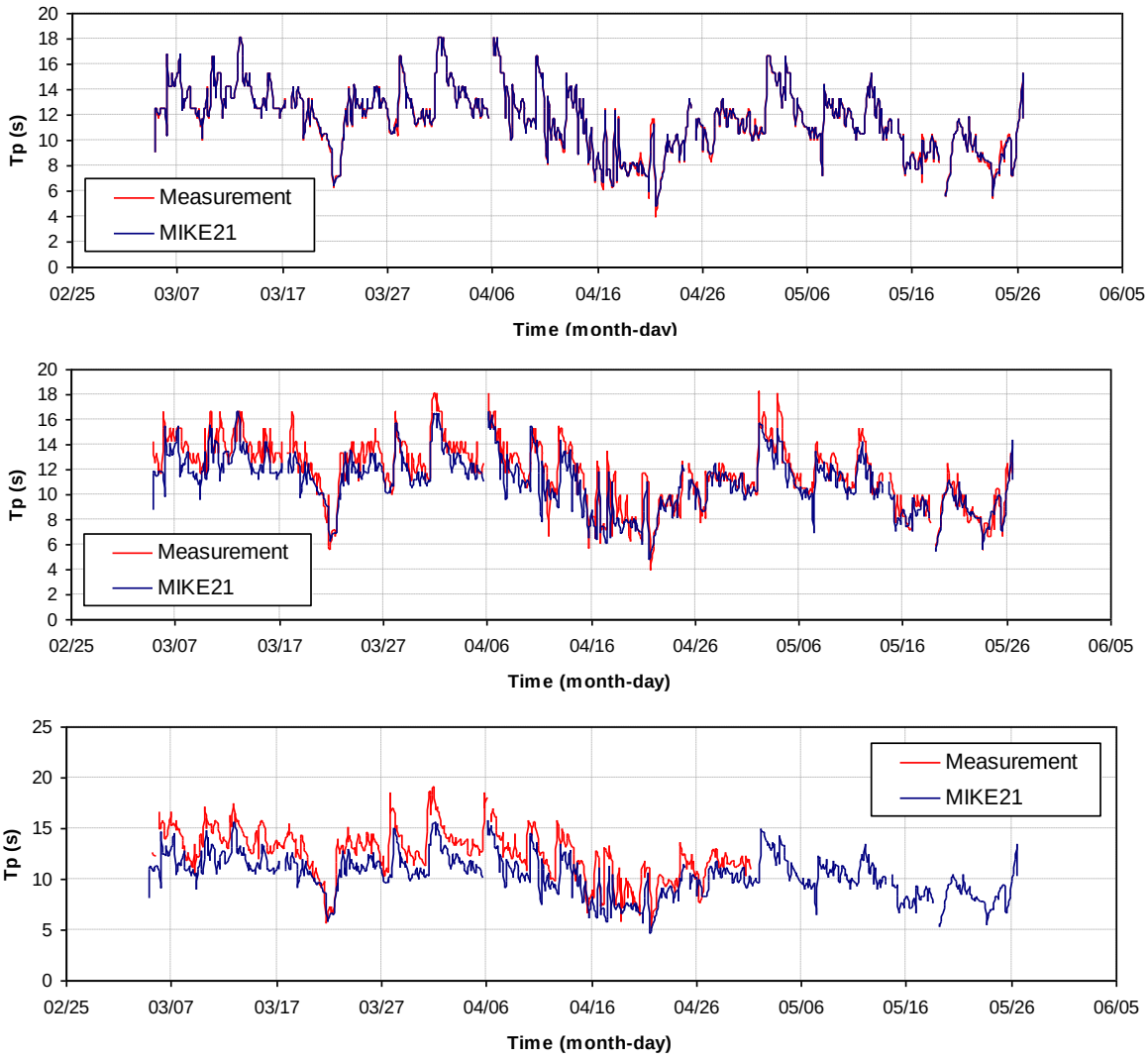

Figure 59 Peak wave period (T_p) time series: (i) Buoy DW1 offshore buoy (at 70m depth) – upper plot, (ii) Buoy DW2 (20m water depth) – middle plot, and (iii)) Buoy DW3 (12 m depth) – bottom plot. The wind forcing is not included in the modelling.

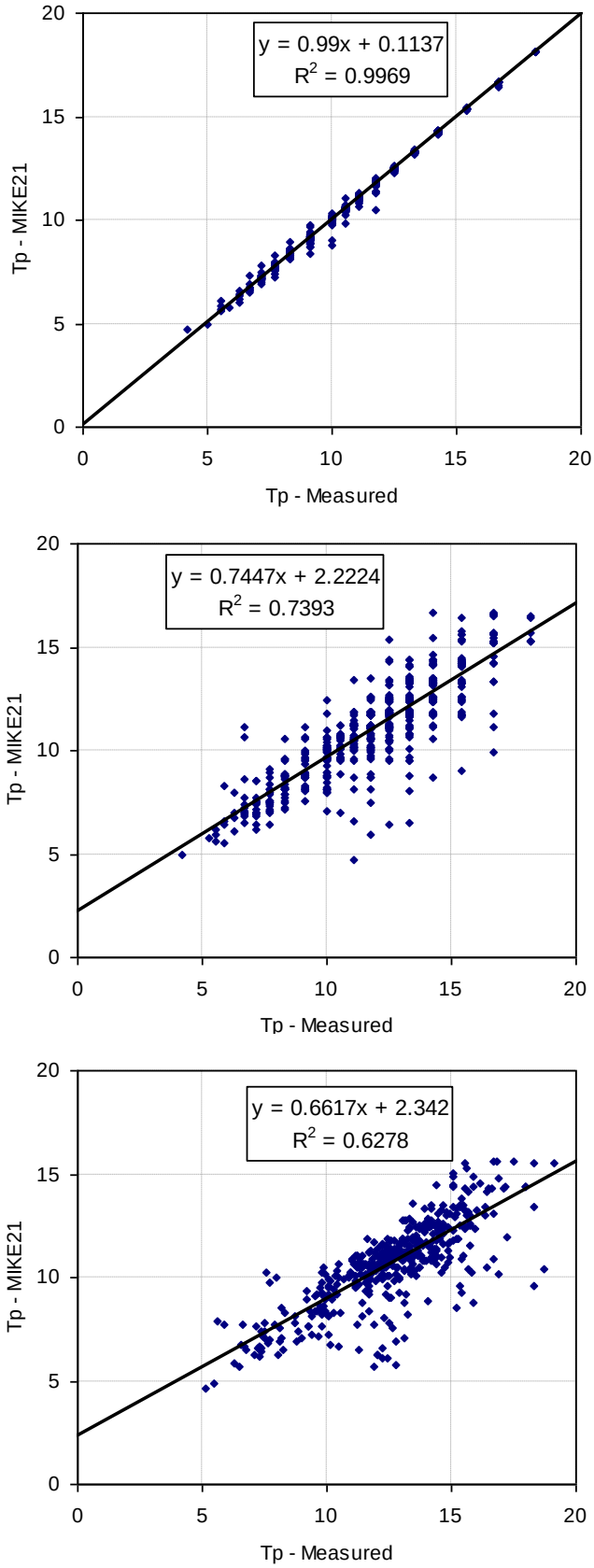

Figure 60 Comparison of peak period (T_p) between measurements and MIKE21 model: (i) Buoy DW1 offshore buoy (at 70m depth) – upper plot, (ii) Buoy DW2 (20m water depth) – middle plot, and (iii) Buoy DW3 (12 m depth) – bottom plot. The wind forcing is not included in the modelling.

4 DISCUSSION

4.1 INTERCOMPARISON OF RESULTS

The correlation coefficient *R* obtained between measured buoy data and wave model output for various wave parameters are listed in Table 4. In general, the *R* values are above 0.8 indicating a very good correlation.

SWAN is a very user-friendly model in the sense that it offers many options to play rapidly with the first simulations (runs). For the case of Figueira da Foz, it allows to realise a sequence of stationary computations in the non stationary mode. When the domain is relatively small, as considered here, this option is relevant and permits to save computational time.

TOMAWAC modelling offers a good representation of wave propagation at Figueira da Foz. Better fits may be obtained by tuning the numerous parameters of the code.

MIKE21 produces similar results to SWAN and TOMWAC and its user friendly graphical pre-processing and post-processing aids much in quicker visualisation and plotting output parameters. Although this model could be tuned to produce more accurate results, running with default model parameters resulted in slightly smaller *R* value for peak wave period at 12m depth.

In terms of computational efficiency, SWAN model prevails since it allows realising a sequence of stationary computations in the non stationary mode. This option is not available in TOMAWAC. The main interest of TOMAWAC is its integration into the TELEMAC system and the coupling easily achieved between hydrodynamic, sediment transport and wave modules.

Including wind into the wave models does not seem to greatly influence the output wave parameters and the reason could be that within the small computational area selected, the energy transfer from wind has little effect on wave generation and propagation.

The location of Figueira da Foz is rather simple in the sense that the bathymetry is smooth and coastal geometry nearly linear. This explains the good agreement between the model results and measured data, despite the use of coarse bathymetric data. However, it is apparent from the correlation plots that there are few differences between three model's outputs which could be attributed to their individual formulations and input model parameters (coefficients) selected for the simulations.

Table 4 Correlation coefficients for wave parameters

		SWAN (unstructured) Linear correlation, R		**TOMAWAC Linear correlation, R**		**SWAN (regular grid) Linear correlation, R**			**MIKE21 Linear correlation, R**
Wave Parameter	**Buoy**	**No wind**	**With wind**	**No wind**	**With wind**	**Input1**	**Input2**	**Input3**	
H_{m0}	DW2	0.98	0.97	0.95	0.95	0.96	0.95	0.96	0.98
H_{m0}	DW3	0.95	0.95	0.91	0.91	0.96	0.94	0.94	0.94
M_{dir}	DW2	0.98	0.97	0.97	0.97	0.94	0.83	0.86	0.97
T_p	DW2	0.88	0.89	0.84	0.84	-	-	-	0.86
T_p	DW3	0.86	0.86	0.81	0.82	-	-	-	0.81
T_{m02}	DW2	0.96	0.89	0.92	0.92	0.94	0.91	0.88	-
T_{m02}	DW3	0.93	0.93	0.79	0.83	0.87	0.83	0.853	-

5 REFERENCES

1. SWAN user guide, http://vlm089.citg.tudelft.nl/swan/index.htm
2. TOMAWAC, http://actimar.free.fr/mambo/index.php?option=com_content&task=view&id=159&Itemid=215&lang=en
3. MIKE21 User guide (2008), http://www.mikebydhi.com/